Variational formulation of a quantitative phase-field model for nonisothermal solidification in a multicomponent alloy

Munekazu Ohno,[1] Tomohiro Takaki,[2] and Yasushi Shibuta[3]

[1]*Division of Materials Science and Engineering, Faculty of Engineering, Hokkaido University, Kita 13 Nishi 8, Kita-ku, Sapporo, Hokkaido 060-8628, Japan*

[2]*Faculty of Mechanical Engineering, Kyoto Institute of Technology, Matsugasaki, Sakyo-ku, Kyoto 606-8585, Japan*

[3]*Department of Materials Engineering, The University of Tokyo, 7-3-1 Hongo, Bunkyo-ku, Tokyo 113-8656, Japan*

(Received 9 May 2017; published 20 September 2017)

A variational formulation of a quantitative phase-field model is presented for nonisothermal solidification in a multicomponent alloy with two-sided asymmetric diffusion. The essential ingredient of this formulation is that the diffusion fluxes for conserved variables in both the liquid and solid are separately derived from functional derivatives of the total entropy and then these fluxes are related to each other on the basis of the local equilibrium conditions. In the present formulation, the cross-coupling terms between the phase-field and conserved variables naturally arise in the phase-field equation and diffusion equations, one of which corresponds to the antitrapping current, the phenomenological correction term in early nonvariational models. In addition, this formulation results in diffusivities of tensor form inside the interface. Asymptotic analysis demonstrates that this model can exactly reproduce the free-boundary problem in the thin-interface limit. The present model is widely applicable because approximations and simplifications are not formally introduced into the bulk's free energy densities and because off-diagonal elements of the diffusivity matrix are explicitly taken into account. Furthermore, we propose a nonvariational form of the present model to achieve high numerical performance. A numerical test of the nonvariational model is carried out for nonisothermal solidification in a binary alloy. It shows fast convergence of the results with decreasing interface thickness.

DOI: 10.1103/PhysRevE.96.033311

I. INTRODUCTION

Solidification in practical alloys is generally a multiphysics problem involving multicomponent solute diffusion, heat diffusion, and fluid dynamics. The understanding and control of solidification microstructures require the multiphysics nature to be taken into account in detail. The phase-field model is a viable computational tool for describing microstructural evolution processes in multiphysics phenomena including solidification [1–4]. The most appealing feature of this diffuse interface approach is that explicit tracking of a moving interface can be avoided by introducing an order parameter called a phase-field variable ϕ, which takes different constant values in different bulks and exhibits rapid spatial variation inside the interface.

Another important feature of the phase-field model is that it can be constructed on the basis of a variational principle of nonequilibrium thermodynamics. More precisely, once the thermodynamic potential (free energy or entropy) of a system is defined in the form of a Ginzburg–Landau type functional, the time evolution equations for ϕ and the related state variables (composition, temperature, etc.) can be obtained from the variational derivative of the thermodynamic potential [5–10]. Such a formulation ensures a solid linkage between the phase-field model and the thermodynamics. Moreover, it provides a basic recipe for generalization of the model to a variety of important application fields. However, models constructed in the variational manner are generally not suitable for the quantitative description of microstructural processes involving diffusive transport such as solute and heat diffusion. This problem arises because the conventional models can be mapped onto the corresponding free-boundary problem only in the limit of vanishing interface thickness W (sharp-interface limit), whereas a finite thickness must be employed in simulations of this diffuse interface approach. It has been demonstrated that the models suffer from abnormal interface effects that scale with W [11].

The development of quantitative phase-field models opened the way for quantitative simulations of solidification microstructures [12–17]. These models were developed to reproduce the solution of the free-boundary problem in the thin-interface limit, where W is taken to be smaller than any length scale of the microstructure but much larger than the atomistic scale. The first quantitative model was proposed for solidification in a pure substance with equal thermal diffusivity in the solid and liquid (symmetric diffusion) [12]. In this case, the abnormal interface effects can be eliminated by imposing certain symmetries on model functions (polynomial functions of ϕ) and by revising the relation between a model parameter (phase-field mobility) and measurable quantities. A quantitative model was later developed for isothermal solidification in a dilute binary alloy with negligible solid diffusion (one-sided diffusion) [13]. The one-sided case involves an additional interface effect that originates from the discontinuity of the diffusion potential in the interface. This additional effect is proportional to the interface velocity and is removed by introducing a correction term of the diffusion flux proportional to the interface velocity, i.e., $\partial_t \phi$ [14]. This term is called the antitrapping current, which represents the coupling between ϕ and the conserved variable. The one-sided model was extended to deal with nonisothermal [15] and two-phase solidification [16] in a binary alloy and isothermal solidification in a multicomponent alloy [17]. The simulation results of quantitative models rapidly converge to unique values (the solutions of the free-boundary problem) with decreasing W,

indicating good numerical performance [11,14]. Quantitative phase-field models are increasingly utilized in studies on the formation processes of solidification microstructures [18–23].

There is a difficulty in developing the quantitative phase-field model for alloy solidification with unequal diffusivities in the solid and liquid (asymmetric diffusion). The asymmetric two-sided diffusion involves additional abnormal interface effects proportional to the diffusion flux and hence not all interface effects can be eliminated by the antitrapping current. An assumption on the diffusion flux near the interface was accordingly imposed in the early quantitative models for two-sided diffusion [24–27]. In a recent study on the solidification of a pure substance with asymmetric diffusion [28], Boussinot and Brener demonstrated that all abnormal interface effects can be successfully removed by introducing a new coupling term into the ϕ equation in addition to the antitrapping current. Namely, they reported the important finding that the quantitative phase-field modeling of two-sided asymmetric diffusion can be accomplished by introducing cross-coupling terms between ϕ and the conserved variable into the time evolution equations of both variables.

The antitrapping current was introduced in a phenomenological manner in early works on quantitative phase-field modeling [13–17,24–27]. This is a correction term formulated based on the result of asymptotic analysis of the model equations. Importantly, it cannot be naturally derived in a variational manner from the functional derivative of the thermodynamic potential. In this regard, the early quantitative phase-field models do not have a sound theoretical basis of nonequilibrium thermodynamics. Progress has recently been made regarding this matter. In the conventional variational formulation, the diffusion flux is related to the functional derivative of the thermodynamic potential with respect to the only corresponding conserved variable (composition or energy field). In Refs. [28–30], on the other hand, the kinetic cross coupling between ϕ and the conserved variable is taken into account by introducing the corresponding transport coefficients. Then, the coupling term in the diffusion equation is regarded as the antitrapping current. In this approach, a coupling term is also introduced into the ϕ equation to maintain the Onsager's symmetry. As described above, this new coupling term in the ϕ equation plays an important role in eliminating the interface effects in asymmetric diffusion [28]. This approach thereby enables the variational derivation of a quantitative phase-field model. As discussed in Ref. [28], however, the ratio of solid diffusivity to liquid diffusivity in this approach is limited to a certain small range to ensure the positive entropy production rate. Accordingly, there is a limitation in range of application of this approach. In addition, the cross-coupling terms must carefully be tuned on the basis of asymptotic analysis of the model equations in this approach, which may not always be straightforward when the approach is extended to describe new systems. These facts indicate the necessity for a further attempt to develop an approach of variational formulation of quantitative phase-field models.

A different method for the variational formulation of a quantitative phase-field model was recently proposed for isothermal solidification in a dilute binary alloy [31]. In this formulation, the kinetic cross coupling is not directly introduced and new transport coefficients therefore do not need to be taken into account. This formulation is based on the so-called two-phase approach, where the composition and thermodynamic quantities in the solid and liquid are separately defined and the interface is treated as a mixture of two phases [10,32]. In the conventional variational derivation, a local equilibrium condition (more precisely, the condition of equal diffusion potentials) is imposed on the thermodynamic potential, which results in mutual dependence of the solid and liquid compositions. Then the time evolution equations of ϕ and the single composition are derived from the thermodynamic potential. This conventional procedure results in a standard phase-field model in which the antitrapping current does not exist. Note that in reality, the local equilibrium condition should essentially be realized as a result of the kinetics [33]. Therefore, in the previous work [31], the diffusion fluxes of both the solid and liquid compositions were first derived in a variational manner and then the local equilibrium condition was applied to the diffusion fluxes. This is more natural than the conventional method of variational formulation from the viewpoint of thermodynamics and it actually yields a quantitative phase-field model for a two-sided case. The cross-coupling terms in the ϕ equation and diffusion equation naturally emerge in this variational formulation and the forms of the cross-coupling terms are automatically determined. Furthermore, there is no limitation on the diffusivity ratio. Asymptotic analysis showed that this model can reproduce the solution of the free-boundary problem in the thin-interface limit. In the present paper, this approach is called the two-phase variational approach to distinguish it from the approach based on the direct introduction of kinetic cross-coupling with the additional transport coefficients [28–30].

In the previous study on the two-phase variational approach [31], the focus was directed at a simple case, isothermal solidification in a dilute binary alloy where the independent variables are only ϕ and a single composition field. To establish this approach and verify its usefulness, it is indispensable to tackle more general cases such as nonisothermal solidification in multicomponent alloys. Furthermore, such an attempt is essential for widening the range of applications of quantitative phase-field simulations. So far, quantitative models have been developed only for some specific systems. Several simplifications and approximations are employed for bulk's quantities in these models such as a constant heat capacity, constant diffusivity, a linearized driving force, and so forth. This is because it is not straightforward to develop a quantitative model in the conventional manner without several simplifications and approximations.

In this paper, we show the variational formulation of a quantitative phase-field model for nonisothermal solidification in a multicomponent alloy based on the two-phase variational approach. The present model is able to describe two-sided asymmetric diffusion in a system without specific approximations in the forms of bulk's free energy densities and other thermodynamic quantities. In addition, the contributions of off-diagonal elements of the diffusivity matrix are explicitly considered. Hence, this model can be applied to a variety of practical problems. In this paper, we also describe in detail important aspects and consequences of the two-phase variational approach such as the natural derivation of the tensor diffusivity and the proportionality between the phase-field

mobility and interface mobility, which were not clarified in the previous study [31]. This paper is organized as follows. The variational formulation of the quantitative phase-field model is demonstrated in the next section. The essential points of analysis in the thin-interface limit are briefly explained in Sec. III. The model equations are illustrated for some specific cases in Sec. IV, which is followed by the numerical testing of the model in Sec. V. Conclusions are given in Sec. VI.

II. VARIATIONAL FORMULATION BASED ON ENTROPY FUNCTIONAL

A. Entropy functional and time evolution equations

We focus on nonisothermal solidification in a multicomponent alloy consisting of n solute and solvent atoms, i.e., a $n+1$ component system. The phase-field variable ϕ takes values of $+1$ in a solid and -1 in a liquid and it continuously changes from $+1$ to -1 inside the solid-liquid interface. In this formulation, we employ the two-phase approach, in which the thermodynamic quantities in the solid and liquid are separately defined and the interface is described as a mixture of two phases [10,32,34,35]. As briefly mentioned in the previous section, one of the important points in the present formulation is that the diffusion fluxes for the conserved variables in both the solid and liquid are first formulated and then they are related to each other by introducing the local equilibrium conditions. This is in contrast to the conventional procedure, where the local equilibrium condition is imposed on the thermodynamic potential before the formulation of the diffusion flux.

A free energy functional was employed as the fundamental thermodynamic potential in the previous variational formulation for isothermal solidification [31]. On the other hand, the entropy is the fundamental thermodynamic potential for nonisothermal solidification processes [5,7]. In this study, the entropy functional is defined as

$$S = \int \left(-\frac{\varepsilon_{\rm ent}^2}{2}(\nabla\phi)^2 - \omega_{\rm ent} f_{dw}(\phi) + \frac{1+g(\phi)}{2} s_{s,\rm bulk}(e_s,\{c_{s,i}\}) + \frac{1-g(\phi)}{2} s_{l,\rm bulk}(e_l,\{c_{l,i}\}) \right) dv, \tag{1}$$

where $\varepsilon_{\rm ent}$ and $\omega_{\rm ent}$ are constants related to the interfacial energy and interface thickness. For simplicity, the anisotropy of the interface energy is omitted in the discussion. In Eq. (1), $f_{dw}(\phi)$ is the double-well function given as

$$f_{dw}(\phi) = \tfrac{1}{4}(1-\phi^2)^2. \tag{2}$$

$g(\phi)$ is a monotonically increasing function and it should be an odd function of ϕ. Among several possible forms for $g(\phi)$, the following function is used in this study:

$$g(\phi) = \frac{15}{8}\left(\phi - \frac{2}{3}\phi^3 + \frac{\phi^5}{5}\right). \tag{3}$$

In Eq. (1), $s_{p,\rm bulk}$ is the bulk's entropy density of phase p, which is a function of the energy density e_p and solute compositions $\{c_{p,i}\}$, where i specifies the type of solute atom ($i \leqslant n$). When the solid-liquid interface is stationary, e_p and $c_{p,i}$ should obey the following conservation laws:

$$\partial_t e_p + \nabla\cdot\mathbf{J}_{p,e} = 0, \tag{4}$$

$$\partial_t c_{p,i} + \Omega\nabla\cdot\mathbf{J}_{p,i} = 0, \tag{5}$$

where Ω is the molar volume, which is assumed constant in this study, $\mathbf{J}_{p,e}$ is the energy flux in phase p, and $\mathbf{J}_{p,i}$ is the diffusion flux of solute i in phase p. When the interface migrates, e_p and $c_{p,i}$ are not conserved variables because the release of latent heat and redistribution of solutes take place in the interface. Such effects can be described by introducing reaction terms into Eqs. (4) and (5) [31]. On the other hand, when the interface migrates, one should consider the conservation of the local molar energy e and the local composition c_i of solute i, which are respectively given as

$$e = \frac{1+g}{2}e_s + \frac{1-g}{2}e_l, \tag{6}$$

$$c_i = \frac{1+g}{2}c_{s,i} + \frac{1-g}{2}c_{l,i}. \tag{7}$$

The conservation laws of these quantities are expressed as

$$\partial_t e + \nabla\cdot\mathbf{J}_e = \partial_t e + \nabla\cdot\left(\frac{1+g}{2}\mathbf{J}_{s,e} + \frac{1-g}{2}\mathbf{J}_{l,e}\right) = 0, \tag{8}$$

$$\partial_t c_i + \Omega\nabla\cdot\mathbf{J}_i = \partial_t c_i + \Omega\nabla\cdot\left(\frac{1+g}{2}\mathbf{J}_{s,i} + \frac{1-g}{2}\mathbf{J}_{l,i}\right) = 0. \tag{9}$$

As can be understood from Eqs. (4)–(9), the energy and compositions obey similar relations. For convenience, we employ the notations of $c_{p,n+1} = \Omega e_p$, $c_{n+1} = \Omega e$, $\mathbf{J}_{p,n+1} = \mathbf{J}_{p,e}$, and $\mathbf{J}_{n+1} = \mathbf{J}_e$ in the following discussion.

Next, we consider the time change in the entropy functional S. Equations (6) and (7) are taken into account by using the Lagrange multipliers Λ_i as follows:

$$\bar{S} = S + \int \sum_{i=1}^{n+1} \Lambda_i \left(\frac{1+g}{2}c_{s,i} + \frac{1-g}{2}c_{l,i} - c_i\right) dv. \tag{10}$$

Then, the time derivative of $\bar{S}$ is given as

$$\frac{d\bar{S}}{dt} = \int \left(\frac{\delta S}{\delta\phi}\partial_t\phi + \sum_{i=1}^{n+1}\left[\frac{\delta S}{\delta c_{s,i}}\partial_t c_{s,i} + \frac{\delta S}{\delta c_{l,i}}\partial_t c_{l,i}\right]\right) dv + \int \sum_{i=1}^{n+1} \Lambda_i \left(\frac{1+g}{2}\partial_t c_{s,i} + \frac{1-g}{2}\partial_t c_{l,i} - \partial_t c_i + (c_{s,i} - c_{l,i})\frac{g'}{2}\partial_t\phi\right) dv. \tag{11}$$

Here, the terms proportional to $\partial_t c_{p,i}$ indicate the contributions due to time changes of solute compositions and energy without the change of ϕ, i.e., without the motion of interface. Hence, $\partial_t c_{p,i}$ should be represented by Eqs. (4) and (5) [36]. Then, by

substituting Eqs. (4), (5), (8), and (9) into Eq. (11), one obtains

$$\frac{d\bar{S}}{dt} = \int \left\{ \left(\frac{\delta S}{\delta \phi} + \frac{g'}{2} \sum_{i=1}^{n+1} \Lambda_i (c_{s,i} - c_{l,i}) \right) \partial_t \phi - \Omega \sum_{i=1}^{n+1} \left[\frac{\delta S}{\delta c_{s,i}} \nabla \cdot \mathbf{J}_{s,i} + \frac{\delta S}{\delta c_{l,i}} \nabla \cdot \mathbf{J}_{l,i} \right] + \Omega \frac{g'}{2} \sum_{i=1}^{n+1} \Lambda_i (\mathbf{J}_{s,i} - \mathbf{J}_{l,i}) \cdot \nabla \phi \right\} dv. \tag{12}$$

Using the divergence theorem, this equation is rewritten as

$$\frac{d\bar{S}}{dt} = -\int \mathbf{J}_{\text{ent}} \cdot \mathbf{n}_{\text{sys}} ds_a + \int \sigma_{\text{ent}} dv, \tag{13}$$

where $\mathbf{n}_{\text{sys}}$ is the unit vector normal to the surface of the whole system, ds_a indicates the unit surface area, and

$$\mathbf{J}_{\text{ent}} = \Omega \sum_{i=1}^{n+1} \left[\frac{\delta S}{\delta c_{s,i}} \mathbf{J}_{s,i} + \frac{\delta S}{\delta c_{l,i}} \mathbf{J}_{l,i} \right], \tag{14}$$

$$\sigma_{\text{ent}} = \left(\frac{\delta S}{\delta \phi} + \frac{g'}{2} \sum_{i=1}^{n+1} \Lambda_i (c_{s,i} - c_{l,i}) \right) \partial_t \phi + \Omega \sum_{i=1}^{n+1} \left[\left(\nabla \frac{\delta S}{\delta c_{s,i}} + \frac{g'}{2} \Lambda_i \nabla \phi \right) \cdot \mathbf{J}_{s,i} + \left(\nabla \frac{\delta S}{\delta c_{l,i}} - \frac{g'}{2} \Lambda_i \nabla \phi \right) \cdot \mathbf{J}_{l,i} \right]. \tag{15}$$

Note that

$$\frac{\delta S}{\delta c_{s,i}} = -\frac{1+g}{2} \frac{\Delta \mu_{s,i}}{T_s}, \tag{16}$$

$$\frac{\delta S}{\delta c_{l,i}} = -\frac{1-g}{2} \frac{\Delta \mu_{l,i}}{T_l}, \tag{17}$$

for $i \leqslant n$. Here, $\Delta \mu_{p,i}$ is the difference in the chemical potential between solute atom i and a solvent atom in phase p and T_p is the temperature in phase p. In the case of $i = n + 1$,

$$\frac{\delta S}{\delta e_s} = \frac{1+g}{2} \frac{1}{T_s}, \tag{18}$$

$$\frac{\delta S}{\delta e_l} = \frac{1-g}{2} \frac{1}{T_l}. \tag{19}$$

The substitution of Eqs. (16)–(19) into Eq. (14) yields

$$\mathbf{J}_{\text{ent}} = \frac{1+g}{2} \left(\frac{1}{T_s} \mathbf{J}_{s,e} - \frac{1}{T_s} \Omega \sum_{i=1}^{n} \Delta \mu_{s,i} \mathbf{J}_{s,i} \right) + \frac{1-g}{2} \left(\frac{1}{T_l} \mathbf{J}_{l,e} - \frac{1}{T_l} \Omega \sum_{i=1}^{n} \Delta \mu_{l,i} \mathbf{J}_{l,i} \right). \tag{20}$$

The first and second terms of Eq. (20) represent well-known relationships for the entropy fluxes in the solid and liquid, respectively [37]. Therefore, $\mathbf{J}_{\text{ent}}$ is identified as the entropy flux in the two-phase approach. In Eq. (13), accordingly, σ_{ent} corresponds to the entropy production and it should monotonically increase during solidification. σ_{ent} is now rewritten as

$$\sigma_{\text{ent}} = \left(\frac{\delta S}{\delta \phi} + \frac{g'}{2} \sum_{i=1}^{n+1} \Lambda_i (c_{s,i} - c_{l,i}) \right) \partial_t \phi + \sum_{i=1}^{n+1} \left[\left(\nabla_n \frac{\delta S}{\delta c_{s,i}} + \frac{g'}{2} \Lambda_i \nabla \phi \right) \cdot \Omega \mathbf{J}_{s,i}^n + \left(\nabla_n \frac{\delta S}{\delta c_{l,i}} - \frac{g'}{2} \Lambda_i \nabla \phi \right) \cdot \Omega \mathbf{J}_{l,i}^n \right] + \sum_{i=1}^{n+1} \left[\left(\nabla_t \frac{\delta S}{\delta c_{s,i}} \right) \cdot \Omega \mathbf{J}_{s,i}^t + \left(\nabla_t \frac{\delta S}{\delta c_{l,i}} \right) \cdot \Omega \mathbf{J}_{l,i}^t \right], \tag{21}$$

where $\mathbf{J}_{p,i}^n$ and $\mathbf{J}_{p,i}^t$ are the diffusion fluxes of normal and tangential directions to the interface in phase p, respectively. Therefore, $\mathbf{J}_{p,i} = \mathbf{J}_{p,i}^n + \mathbf{J}_{p,i}^t$. ∇_n and ∇_t are operators of the spatial derivative in the normal and tangential directions to the interface, respectively. In writing Eq. (21), we employed the relations $\nabla_n \phi = \nabla \phi$ and $\nabla_t \phi = 0$, which are always valid in this diffuse interface approach. This separation of the diffusion flux was not considered in the previous study [31]. However, the term associated with the Lagrange multiplier is related to the diffusion flux in the only normal direction. Therefore, it is necessary to define the diffusion flux for each direction. As demonstrated later, this separation brings an important consequence that the diffusivity is tensor inside the interface.

The time evolution equation of ϕ and the diffusion fluxes are formulated on the basis of the principle that σ_{ent} given by Eq. (21) is always positive or equal to zero. This can be achieved by introducing phenomenological transport coefficients [5,7,35]. Care must be taken to ensure the following points [31]. The first term in the integrand of Eq. (21) should contribute to the entropy production only inside the interface. This will be automatically satisfied without special care because $\partial_t \phi$ is zero outside the interface, which will be understood from the final form of the time evolution equation. In addition, one must ensure the condition that $\mathbf{J}_{s,i}$ ($\mathbf{J}_{l,i}$) does not contribute to the entropy production in the liquid (solid) phase. This is because $\mathbf{J}_{s,i}$ ($\mathbf{J}_{l,i}$) is a fictitious flux in the liquid (solid) phase. However, this condition is not automatically realized. As discussed later, the local equilibrium conditions establish the relation between $c_{s,i}$ and $c_{l,i}$ in the interface and also in both bulk phases. Then, $\mathbf{J}_{s,i}$ ($\mathbf{J}_{l,i}$) changes in accordance with $\mathbf{J}_{l,i}$ ($\mathbf{J}_{s,i}$). Therefore, $\mathbf{J}_{s,i}$ ($\mathbf{J}_{l,i}$) is finite even in the liquid (solid). This is a situation commonly involved in the two-phase approaches. Hence, in order for $\mathbf{J}_{s,i}$ ($\mathbf{J}_{l,i}$) not to contribute to the entropy production in the liquid (solid), we consider the following form of σ_{ent}:

$$\sigma_{\text{ent}} = \frac{\partial_t \phi}{M_\phi} \partial_t \phi + \sum_{i=1}^{n+1} \left[\left(\frac{1+g}{2} \sum_{j=1}^{n+1} M_{s,ij}^{-1} \Omega \mathbf{J}_{s,j}^n \right) \cdot \Omega \mathbf{J}_{s,i}^n + \left(\frac{1-g}{2} \sum_{j=1}^{n+1} M_{l,ij}^{-1} \Omega \mathbf{J}_{l,j}^n \right) \cdot \Omega \mathbf{J}_{l,i}^n \right]$$

$$+\sum_{i=1}^{n+1}\left[\left(\frac{1+g}{2}\sum_{j=1}^{n+1}M_{s,ij}^{-1}\Omega\mathbf{J}_{s,j}^{t}\right)\cdot\Omega\mathbf{J}_{s,i}^{t}+\left(\frac{1-g}{2}\sum_{j=1}^{n+1}M_{l,ij}^{-1}\Omega\mathbf{J}_{l,j}^{t}\right)\cdot\Omega\mathbf{J}_{l,i}^{t}\right], \tag{22}$$

where M_ϕ is the phase-field mobility with $M_\phi > 0$ and $M_{p,ij}$ is the i-j element of the transport coefficient matrix $\mathbf{M}_p$ which is a positive-definite matrix in phase p, ensuring that $\sigma_{\text{ent}} \geqslant 0.M_{p,ij}^{-1}$ is the i-j element of the inverse matrix of $\mathbf{M}_p$. $\mathbf{M}_p$ and thus $\mathbf{M}_p^{-1}$ are symmetric matrices and this property is utilized in the following discussion without explicitly mentioning it. By comparing Eqs. (21) and (22), one can obtain the following equations:

$$\frac{\partial_t\phi}{M_\phi}=\frac{\delta S}{\delta\phi}+\frac{g'}{2}\sum_{i=1}^{n+1}\Lambda_i(c_{s,i}-c_{l,i}), \tag{23}$$

$$\frac{1+g}{2}\sum_{j=1}^{n+1}M_{s,ij}^{-1}\Omega\mathbf{J}_{s,j}^{n}=\nabla_n\frac{\delta S}{\delta c_{s,i}}+\frac{g'}{2}\Lambda_i\nabla\phi, \tag{24}$$

$$\frac{1-g}{2}\sum_{j=1}^{n+1}M_{l,ij}^{-1}\Omega\mathbf{J}_{l,j}^{n}=\nabla_n\frac{\delta S}{\delta c_{l,i}}-\frac{g'}{2}\Lambda_i\nabla\phi, \tag{25}$$

$$\frac{1+g}{2}\sum_{j=1}^{n+1}M_{s,ij}^{-1}\Omega\mathbf{J}_{s,j}^{t}=\nabla_t\frac{\delta S}{\delta c_{s,i}}, \tag{26}$$

$$\frac{1-g}{2}\sum_{j=1}^{n+1}M_{l,ij}^{-1}\Omega\mathbf{J}_{l,j}^{t}=\nabla_t\frac{\delta S}{\delta c_{l,i}}. \tag{27}$$

B. Lagrange multipliers and local equilibrium conditions

The substitution of Eqs. (4)–(7) into Eqs. (8) and (9) yields the following equation, which corresponds to the Stefan condition expressed in the diffuse interface approach [31,35]:

$$(c_{s,i}-c_{l,i})\partial_t\phi=-\Omega\left(\mathbf{J}_{s,i}^{n}-\mathbf{J}_{l,i}^{n}\right)\cdot\nabla\phi. \tag{28}$$

By substituting the diffusion fluxes given by Eqs. (24) and (25) into Eq. (28), one finds that

$$\Lambda_i\frac{g'}{2}\nabla\phi=-\frac{1-g}{2}\sum_{j,k}M_{c,ij}^{-1}M_{s,jk}\nabla_n\frac{\delta S}{\delta c_{s,k}}+\frac{1+g}{2}\sum_{j,k}M_{c,ij}^{-1}M_{l,jk}\nabla_n\frac{\delta S}{\delta c_{l,k}}-\frac{1-g^2}{4|\nabla\phi|}\sum_{j}M_{c,ij}^{-1}(c_{s,j}-c_{l,j})\partial_t\phi\frac{\nabla\phi}{|\nabla\phi|}, \tag{29}$$

where $M_{c,ij}^{-1}$ is the inverse of the following matrix:

$$M_{c,ij}=\frac{1-g}{2}M_{s,ij}+\frac{1+g}{2}M_{l,ij}. \tag{30}$$

The time evolution equation of ϕ can be obtained by substituting Eq. (29) into Eq. (23). Also, diffusion fluxes can be expressed by substituting Eq. (29) into Eqs. (24) and (25). Then, by using Eqs. (4) and (5) with the addition of appropriate reaction terms, one can formulate the diffusion equations for $c_{s,i}$ and $c_{l,i}$ separately. Here, it is important to note that the local equilibrium condition is realized for slow solidification processes in which nonequilibrium effects such as solute trapping are negligible. As discussed by Hillert [33], transinterface diffusion, which redistributes solute atoms between the solid and liquid in the interface, is usually a very fast process that results in the reduction of a part of the free energy change associated with the solidification. Then, in the slow solidification process, the diffusion potential in the solid becomes identical to that in the liquid. This corresponds to the local equilibrium condition. In Kim, Kim, and Suzuki's model [10], this condition is introduced into the free energy functional and then the time evolution equations are derived. In the present formulation, on the other hand, Eqs. (23)–(27) were derived without the local equilibrium condition. In the case of a nonisothermal process, which is our main concern, the condition of equal diffusion potential can be expressed as follows:

$$\frac{\partial s_{s,\text{bulk}}}{\partial c_{s,i}}=\frac{\partial s_{l,\text{bulk}}}{\partial c_{l,i}}=\Delta s_{c,i}\ \text{for}\ i\ \leqslant n+1. \tag{31}$$

More specifically,

$$\frac{\partial s_{s,\text{bulk}}}{\partial e_s}=\frac{\partial s_{l,\text{bulk}}}{\partial e_l}. \tag{32}$$

Hence,

$$\frac{1}{T_s}=\frac{1}{T_l}=\frac{1}{T}. \tag{33}$$

For the solute,

$$\frac{\Delta\mu_{s,i}}{T_s}=\frac{\Delta\mu_{l,i}}{T_l}\ \text{for}\ i\ \leqslant n. \tag{34}$$

When Eq. (33) is satisfied, Eq. (34) is equivalent to

$$\Delta\mu_{s,i}=\Delta\mu_{l,i}=\Delta\mu_{c,i}\ \text{for}\ i\ \leqslant n. \tag{35}$$

In the present modeling of slow solidification, instead of solving the diffusion equations of $c_{s,i}$ and $c_{l,i}$ separately, we introduce the local equilibrium conditions, Eqs. (33) and (35). Then, by substituting Eqs. (16)–(19) into Eq. (29) and also by considering Eqs. (33) and (35), the Lagrange multiplier Λ_i is rewritten as

$$\Lambda_i\frac{g'}{2}\nabla\phi=-\frac{g'}{2}\nabla\phi\Delta s_{c,i}-\frac{1-g^2}{4}\sum_{j,k}M_{c,ij}^{-1}(M_{s,jk}-M_{l,jk})\nabla_n(\Delta s_{c,k})-\frac{1-g^2}{4|\nabla\phi|}\sum_{j}M_{c,ij}^{-1}(c_{s,j}-c_{l,j})\,\partial_t\phi\frac{\nabla\phi}{|\nabla\phi|}. \tag{36}$$

The second term on the right-hand side of Eq. (36) is the origin of the cross-coupling term in the ϕ equation, while the third term yields the antitrapping current in the diffusion equations as shown below. Note that $c_{s,i}$ is now related to $\{c_{l,i}\}$ such that Eqs. (33) and (35) are satisfied. Therefore, the independent variables are ϕ and $\{c_{l,i}\}$ in this model.

C. Time evolution equation for ϕ

The substitution of Eq. (36) into Eq. (23) yields

$$\frac{1}{\widetilde{M}_\phi}\partial_t\phi = \varepsilon_{\rm ent}^2\nabla^2\phi - \omega_{\rm ent}f'_{dw} + \frac{g'}{2}\left(s_{s,\rm bulk} - s_{l,\rm bulk} - \sum_{i=1}^{n+1}(c_{s,i}-c_{l,i})\Delta s_{c,i}\right) - \frac{1-g^2}{4|\nabla\phi|}\sum_{i,j,k}(c_{s,i}-c_{l,i})M_{c,ij}^{-1}(M_{s,jk}-M_{l,jk})\nabla_n(\Delta s_{c,k})\cdot\frac{\nabla\phi}{|\nabla\phi|}, \tag{37}$$

where

$$\frac{1}{\widetilde{M}_\phi} = \frac{1}{M_\phi} + \frac{1-g^2}{4|\nabla\phi|^2}\sum_{i,j}(c_{s,i}-c_{l,i})M_{c,ij}^{-1}(c_{s,j}-c_{l,j}). \tag{38}$$

The third term on the right-hand side of Eq. (37) is associated with the driving force for the migration of the solid-liquid interface. It is rewritten as

$$\begin{aligned} s_{s,\rm bulk} - s_{l,\rm bulk} - \sum_{i=1}^{n+1}(c_{s,i}-c_{l,i})\Delta s_{c,i} &= -\frac{f_{s,\rm bulk} - e_s - f_{l,\rm bulk} + e_l}{T} - \sum_{i=1}^{n+1}(c_{s,i}-c_{l,i})\Delta s_{c,i} \\ &= -\frac{1}{T}\left(f_{s,\rm bulk} - f_{l,\rm bulk} - \sum_{i=1}^{n}(c_{s,i}-c_{l,i})\Delta\mu_{c,i}\right) = -\frac{\Delta G_{\rm driv}}{T}, \end{aligned} \tag{39}$$

where $f_{p,\rm bulk}$ is the bulk's free energy density of phase p. The driving force is important only inside the interface, where the temperature does not significantly change. Hence, T in the denominator of Eq. (39) is approximated as a constant T_0, which is called the interface temperature in this study. Then, by multiplying both sides of Eq. (37) by T_0, it is rewritten as

$$\frac{T_0}{\widetilde{M}_\phi}\partial_t\phi = \varepsilon^2\nabla^2\phi - \omega\, f'_{dw} - \frac{g'}{2}\Delta G_{\rm driv} - \frac{1-g^2}{4|\nabla\phi|}T_0\sum_{i,j,k}(c_{s,i}-c_{l,i})M_{c,ij}^{-1}(M_{s,jk}-M_{l,jk})\nabla_n(\Delta s_{c,k})\frac{\nabla\phi}{|\nabla\phi|}, \tag{40}$$

where $\varepsilon^2 = T_0\varepsilon_{\rm ent}^2$ and $\omega = T_0\omega_{\rm ent}$. For convenience, this equation is further modified by considering the steady-state profile of ϕ in the interface. In two-phase equilibrium, $\partial_t\phi$, $\Delta G_{\rm driv}$, and $\nabla(\Delta s_{c,k})$ vanish in Eq. (40) and hence the spatial gradient of ϕ is given by

$$|\nabla\phi| = \frac{\sqrt{2f_{dw}}}{W}, \tag{41}$$

where $W = \varepsilon/\sqrt{\omega}$ is a measure of the thickness of the solid-liquid interface. Also, the interface energy is given as

$$\gamma = I\omega\, W, \tag{42}$$

with $I = 2\sqrt{2}/3$. Using Eqs. (41) and (42), the ϕ equation is finally given as

$$\tau\,\partial_t\phi = W^2\nabla^2\phi - f'_{dw} - \frac{g'}{2}\frac{IW}{\gamma}\Delta G_{\rm driv} - \frac{1-g^2}{4\sqrt{2f_{dw}}}\frac{IW^2}{\gamma}T_0\sum_{i,j,k}(c_{s,i}-c_{l,i})M_{c,ij}^{-1}(M_{s,jk}-M_{l,jk})\nabla_n(\Delta s_{c,k})\cdot\frac{\nabla\phi}{|\nabla\phi|}, \tag{43}$$

where

$$\tau = \frac{T_0}{\omega\widetilde{M}_\phi} = \frac{IW}{\gamma}T_0\left(\frac{1}{M_\phi} + \frac{1-g^2}{8f_{dw}}W^2\sum_{i,j}(c_{s,i}-c_{l,i})M_{c,ij}^{-1}(c_{s,j}-c_{l,j})\right). \tag{44}$$

The last term on the right-hand side of Eq. (43) represents the coupling term, which does not appear in the conventional procedure of the variational formulation. This term plays an important role in eliminating the abnormal interface effects in the thin-interface limit. Moreover, note that τ depends on $\{c_{p,i}\}$, as shown by Eq. (44). In the conventional quantitative models, τ is inversely proportional to the phase-field mobility M_ϕ, which is made $\{c_{p,i}\}$ dependent in accordance with the result of asymptotic analysis [14,24]. In the present variational model, on the other hand, M_ϕ is exactly proportional to the interface mobility defined later. These points will be discussed in more detail in Sec. III.

D. Diffusion equations

The diffusion flux in the solid can be obtained by substituting Eq. (36) into Eq. (24) as follows:

$$\frac{1+g}{2}\Omega\mathbf{J}_{s,i}^{n} = \frac{1+g}{2}\sum_{j} M_{s,ij}\nabla_n(\Delta s_{c,j}) - \frac{1-g^2}{4}\sum_{j,k,k'} M_{s,ij}M_{c,jk}^{-1}(M_{s,kk'} - M_{l,kk'})\nabla_n(\Delta s_{c,k'}) - \frac{1-g^2}{4}\frac{W}{\sqrt{2f_{dw}}}\sum_{j,k} M_{s,ij}M_{c,jk}^{-1}(c_{s,k} - c_{l,k})\,\partial_t\phi\frac{\nabla\phi}{|\nabla\phi|}. \tag{45}$$

Here, Eq. (41) was employed for the last term on the right-hand side of Eq. (45). Similarly, the diffusion flux in the liquid is given as

$$\frac{1-g}{2}\Omega\mathbf{J}_{l,i}^{n} = \frac{1-g}{2}\sum_{j} M_{l,ij}\nabla_n(\Delta s_{c,j}) + \frac{1-g^2}{4}\sum_{j,k,k'} M_{l,ij}M_{c,jk}^{-1}(M_{s,kk'} - M_{l,kk'})\nabla_n(\Delta s_{c,k'}) + \frac{1-g^2}{4}\frac{W}{\sqrt{2f_{dw}}}\sum_{j,k} M_{l,ij}M_{c,jk}^{-1}(c_{s,k} - c_{l,k})\,\partial_t\phi\frac{\nabla\phi}{|\nabla\phi|}. \tag{46}$$

Therefore, one can obtain the following relation:

$$\Omega\mathbf{J}_{i}^{n} = \frac{1+g}{2}\Omega\mathbf{J}_{s,i}^{n} + \frac{1-g}{2}\Omega\mathbf{J}_{l,i}^{n} = \sum_{j} M_{t,ij}\nabla_n(\Delta s_{c,j}) - \frac{1-g^2}{4}\sum_{j,k,k'}(M_{s,ij} - M_{l,ij})M_{c,jk}^{-1}(M_{s,kk'} - M_{l,kk'})\nabla_n(\Delta s_{c,k'}) - \frac{1-g^2}{4}\frac{W}{\sqrt{2f_{dw}}}\sum_{j,k}(M_{s,ij} - M_{l,ij})M_{c,jk}^{-1}(c_{s,k} - c_{l,k})\,\partial_t\phi\frac{\nabla\phi}{|\nabla\phi|}, \tag{47}$$

where $\mathbf{J}_i^n$ is the diffusion flux in the normal direction to the interface and

$$M_{t,ij} = \frac{1+g}{2}M_{s,ij} + \frac{1-g}{2}M_{l,ij}. \tag{48}$$

Note that the following transformation is possible:

$$\sum_{j} M_{t,ij}\nabla_n(\Delta s_{c,j}) = \sum_{j,k,k'} M_{t,ij}M_{c,jk}^{-1}M_{c,kk'}\nabla_n(\Delta s_{c,k'}). \tag{49}$$

Then, Eq. (47) is rewritten as

$$\Omega\mathbf{J}_{i}^{n} = \sum_{k'} M_{n,ik'}\nabla_n(\Delta s_{c,k'}) - \frac{1-g^2}{4}\frac{W}{\sqrt{2f_{dw}}}\sum_{j,k}(M_{s,ij} - M_{l,ij})M_{c,jk}^{-1}(c_{s,k} - c_{l,k})\,\partial_t\phi\frac{\nabla_n\phi}{|\nabla_n\phi|}, \tag{50}$$

where

$$M_{n,ik'} = \sum_{j,k} M_{t,ij}M_{c,jk}^{-1}M_{c,kk'} - \frac{1-g^2}{4}\sum_{j,k}(M_{s,ij} - M_{l,ij})M_{c,jk}^{-1}(M_{s,kk'} - M_{l,kk'}) = \sum_{j,k}\left(\frac{1+g}{2}M_{s,ij}M_{c,jk}^{-1}M_{l,kk'} + \frac{1-g}{2}M_{l,ij}M_{c,jk}^{-1}M_{s,kk'}\right) = \left(\frac{1+g}{2}M_{s,ik'}^{-1} + \frac{1-g}{2}M_{l,ik'}^{-1}\right)^{-1}. \tag{51}$$

This transformation is explained in Appendix A.

The diffusion flux in the tangential direction $\mathbf{J}_i^t$ is obtained from Eqs. (26) and (27) as

$$\Omega\mathbf{J}_{i}^{t} = \frac{1+g}{2}\Omega\mathbf{J}_{s,i}^{t} + \frac{1-g}{2}\Omega\mathbf{J}_{l,i}^{t} = \sum_{j} M_{t,ij}\nabla_t(\Delta s_{c,j}). \tag{52}$$

Therefore,

$$\Omega\mathbf{J}_i = \Omega\left(\mathbf{J}_i^n + \mathbf{J}_i^t\right) = \sum_{j}[M_{n,ij}\mathbf{n}\otimes\mathbf{n} + M_{t,ij}(\mathbf{1} - \mathbf{n}\otimes\mathbf{n})]\nabla(\Delta s_{c,j}) - \frac{1-g^2}{4}\frac{W}{\sqrt{2f_{dw}}}\sum_{j,k}(M_{s,ij} - M_{l,ij})M_{c,jk}^{-1}(c_{s,k} - c_{l,k})\,\partial_t\phi\frac{\nabla\phi}{|\nabla\phi|}, \tag{53}$$

where $\mathbf{n} = -\nabla\phi/|\nabla\phi|$, $\otimes$ represents the tensor product and $\mathbf{1}$ is the unit tensor. Here, we employed $\boldsymbol{\nabla}_n = \mathbf{n}\otimes\mathbf{n}\boldsymbol{\nabla}$ and $\boldsymbol{\nabla}_t = (\mathbf{1}-\mathbf{n}\otimes\mathbf{n})\boldsymbol{\nabla}$.

When the local equilibrium conditions given by Eqs. (33) and (35) are realized, $c_{s,i}$ depends on $\{c_{l,i}\}$ and hence it is written as $c_{s,i} = c_{s,i}(\{c_{l,i}\})$. Then, the time derivative of c_i is given as

$$\partial_t c_i = \partial_t\left(\frac{1+g}{2}c_{s,i} + \frac{1-g}{2}c_{l,i}\right) = \frac{1+g}{2}\sum_j k^c_{ij}\partial_t c_{l,j} + \frac{1-g}{2}\partial_t c_{l,i} + (c_{s,i}-c_{l,i})\frac{g'}{2}\partial_t\phi, \tag{54}$$

where

$$k^c_{ij} = \frac{\partial c_{s,i}}{\partial c_{l,j}} = \sum_k \chi^{-1}_{s,ik}\chi_{l,kj}, \tag{55}$$

with

$$\chi_{p,jk} = \frac{\partial\Delta s_{c,j}}{\partial c_{p,k}} = \frac{\partial^2 s_{p,\mathrm{bulk}}}{\partial c_{p,j}\partial c_{p,k}}. \tag{56}$$

The second equality in Eq. (55) originates from the local equilibrium condition given by Eq. (31). By combining Eqs. (53) and (54), therefore, the diffusion equation is obtained as follows:

$$\frac{1+g}{2}\sum_j k^c_{ij}\partial_t c_{l,j} + \frac{1-g}{2}\partial_t c_{l,i} = \boldsymbol{\nabla}\cdot\left(\sum_j \mathbf{D}_{ij}(\phi)\boldsymbol{\nabla}c_{l,j} + \frac{1-g^2}{4}\frac{W}{\sqrt{2f_{dw}}}\sum_{j,k}(M_{s,ij}-M_{l,ij})M^{-1}_{c,jk}(c_{s,k}-c_{l,k})\,\partial_t\phi\frac{\nabla\phi}{|\nabla\phi|}\right) - (c_{s,i}-c_{l,i})\frac{g'}{2}\partial_t\phi, \tag{57}$$

where $\mathbf{D}_{ij}$ is the diffusivity function given as

$$\mathbf{D}_{ij}(\phi) = -\sum_k M_{n,ik}(\phi)\chi_{l,kj}\mathbf{n}\otimes\mathbf{n} - \sum_k M_{t,ik}(\phi)\chi_{l,kj}(\mathbf{1}-\mathbf{n}\otimes\mathbf{n}). \tag{58}$$

Here, $\mathbf{D}_{ij}(\phi=-1) = -\Sigma_k M_{l,ik}\chi_{l,kj} = D_{l,ij}$ and $\mathbf{D}_{ij}(\phi=+1) = -\Sigma_k M_{s,ik}\chi_{l,kj} = -\Sigma_{k,k'}M_{s,ik}\chi_{s,kk'}k^c_{k'j} = \Sigma_{k'}D_{s,ik'}k^c_{k'j}$ where $D_{l,ij}$ and $D_{s,ij}$ correspond to the diffusivities in the liquid and solid, respectively. Therefore, the present formulation leads to the important consequence that the diffusivity is tensor inside the interface.

It is worth noting the following two points: First, the term proportional to $\partial_t\phi$ in the parenthesis on the right-hand side of Eq. (57) naturally arises in the present formulation. This is the antitrapping current, which corrects the diffusion flux inside the interface, thereby eliminating the abnormal interface effects. Second, the diffusivity is formulated as the tensor given by Eq. (58). This is a consequence of the separate definition of the diffusion fluxes in the normal and tangential directions to the interface as given by Eqs. (24)–(27). In solidification with two-sided asymmetric diffusion, there are abnormal interface effects associated with the diffusion fluxes in the normal and tangential directions. The elimination of such effects requires stringent constraints on the ϕ dependence of the diffusivity [11,24]. It is difficult to satisfy these constraints simultaneously when the scalar diffusivity is employed. On the other hand, such a problem does not occur when the diffusivity is tensor [31,38].

E. Free-boundary problem and summary of the present model

As described above, the model for nonisothermal solidification in a multicomponent alloy was derived in the variational manner. The validity of the model must be carefully investigated by the asymptotic analysis of Eqs. (43) and (57). As described in detail in Sec. III, in the thin-interface limit of this model, the following sharp-interface equations are reproduced:

$$\partial_t c_i = \boldsymbol{\nabla}\cdot\left(\sum_{i=1}^{n+1} D_{p,ij}(\{c_k\})\boldsymbol{\nabla}c_j\right) \text{ in phase } p, \tag{59}$$

$$\Delta G_{\mathrm{driv}}(\{c_k\}) = -\frac{1}{\mu_{\mathrm{int}}}V_n - \gamma\kappa, \tag{60}$$

$$(c_{l,i}-c_{s,i})\,V_n = \sum_{i=1}^{n+1} D_{s,ij}(\{c_k\})\partial_r c_j|^- - \sum_{i=1}^{n+1} D_{l,ij}(\{c_k\})\partial_r c_j|^+, \tag{61}$$

where μ_{int} is the interface mobility and V_n is the interface velocity in the direction normal to the interface. $\partial_r c_j|^+$ ($\partial_r c_j|^-$) represents the spatial gradient of c_j in the normal direction on the liquid (solid) side of the interface. The diffusion in the bulk is represented by Eq. (59), where the off-diagonal elements of the diffusivity matrix and also their dependencies on $\{c_k\}$ are taken into account. Equation (60) indicates the Gibbs-Thomson relation. It is important to point out that approximations and simplifications are not introduced into the forms of the bulk's free energy densities in this model.

Therefore, any type of free energy model, such as the solution model in the CALPHAD method [39], can be employed to describe $\Delta G_{\rm driv}$ in Eq. (60). Finally, Eq. (61) indicates the conservation of solute atoms and energy during the migration of the interface (Stefan condition). These equations are reproduced in the present variational model without any modification. Hence, the present model can be applied to a variety of practical alloy systems.

Note that the model derived in a variational manner does not necessarily exhibit high numerical performance, i.e., fast convergence of the results with decreasing W [12,31]. It is therefore beneficial to develop a nonvariational form of the quantitative model for its practical use. Once the variational model is derived, it is basically straightforward to construct the nonvariational form. In the asymptotic analysis in the next sections, we focus on both the variational and nonvariational models. For this purpose, Eq. (43) is rewritten as

$$\tau\,\partial_t\phi = W^2\nabla^2\phi - f'_{dw} - \widetilde{g}'a_1\frac{W}{d_0}\frac{\Delta G_{\rm driv}}{\chi_e} - \frac{W^2}{d_0}\sum_i a_{c,i}\nabla c_{l,i}\cdot\frac{\nabla\phi}{|\nabla\phi|}, \tag{62}$$

where $\widetilde{g}' = Jg'/2$, $J = 16/15$, $a_1 = I/J$, $d_0 = \gamma/\chi_e$, and χ_e is a constant thermodynamic factor that will be defined later. d_0 is a characteristic length of the microstructural process and it generally corresponds to the capillary length. Also,

$$a_{c,i} = \frac{a_I}{\sqrt{2f_{dw}}}f_{ac}(\phi)\frac{1-h_{\rm inv}}{2}\frac{1+h}{2}\frac{T_0}{\chi_e} \times \sum_{j,k,k'}\Delta C_{k'}M^{-1}_{c,k'k}(M_{l,kj} - M_{s,kj})\chi_{l,ji}, \tag{63}$$

with

$$\Delta C_i = c_{l,i} - c_{s,i}. \tag{64}$$

Here, $a_I = I$, $f_{ac}(\phi) = 1$ and $h = h_{\rm inv} = g$ in the variational model as demonstrated in the previous sections. For the nonvariational model, we append degrees of freedom in the choice of the forms of $f_{ac}(\phi)$, h, and $h_{\rm inv}$. a_I is automatically determined from the forms of $f_{ac}(\phi)$, h, and $h_{\rm inv}$ as shown later. τ is given as

$$\tau = \frac{IW}{d_0}\frac{T_0}{\chi_e}\frac{1}{M_\phi} + a_I\frac{1-h^2}{8f_{dw}}\frac{W^3}{d_0}\frac{T_0}{\chi_e} \times \sum_{i,j} f_{\tau,ij}(\phi)\Delta C_i M^{-1}_{c,ij}\Delta C_j, \tag{65}$$

where $f_{\tau,ij}(\phi) = 1$ in the variational model, while its form is later determined for the nonvariational model.

The diffusion equation (57) is written as

$$\frac{1+h}{2}\sum_j k^c_{ij}\partial_t c_{l,j} + \frac{1-h}{2}\partial_t c_{l,i} = \nabla\cdot\left(\sum_j \mathbf{D}_{ij}\nabla c_{l,j} + a_{AT,i}W\partial_t\phi\frac{\nabla\phi}{|\nabla\phi|}\right) + \Delta C_i\frac{h'}{2}\partial_t\phi, \tag{66}$$

with

$$a_{AT,i} = \frac{1}{\sqrt{2f_{dw}}}\frac{1-h}{2}\frac{1+h_{\rm inv}}{2} \times \sum_{j,k}(M_{l,ij} - M_{s,ij})M^{-1}_{c,jk}\Delta C_k, \tag{67}$$

where g in the variational model is replaced by h and $h_{\rm inv}$. In addition, g in the expressions for $M_{c,ij}$ [Eq. (30)] and $M_{n,ij}$ [Eq. (51)] is replaced by $h_{\rm inv}$, while g in $M_{t,ij}$ [Eq. (48)] is replaced by h. These replacements are made because it was shown by numerical testing of the quantitative models that the numerical performance strongly depends on the order of the polynomial of ϕ [40]. In particular, the function $h_{\rm inv}$ is introduced to avoid a rapid change of $M_{n,ij}$ across the interface, which causes low numerical accuracy [31] as will be explained later.

Let us emphasize the differences between the previous work [31] and the present work. In the previous study on the two-phase variational approach [31], the focus was directed at a simple case, isothermal solidification in a dilute binary alloy where the independent variables are only ϕ and the composition fields of a solute. The formulation started from the free energy functional and a local equilibrium condition equivalent to Eq. (35) was considered. In the present paper, we have focused on nonisothermal solidification in a multicomponent alloy where the independent variables are ϕ, the energy density, and composition fields. The thermodynamic function is the entropy functional and the local equilibrium condition for each diffusion field [Eqs. (33) and (35)] is taken into consideration in the present case. In addition, the contributions of off-diagonal diffusivities are included. In the present case, importantly, the tensor diffusivity is naturally derived as a consequence of separate definitions of diffusion fluxes in normal and tangential directions to the interface. This is in contrast to the previous approach where the natural derivation of tensor diffusivity was not achieved. Note that the present variational model is reduced to the previous variational model of Ref. [31] when isothermal solidification in a dilute binary alloy is considered. However, the nonvariational form proposed in this study is different from those in the previous models. In the present nonvariational models, there are degrees of freedom in choosing the functions $h(\phi)$, $h_{\rm inv}(\phi)$, $f_{ac}(\phi)$, and $f_{\tau,ij}(\phi)$. The nonvariational model can be mapped onto the free-boundary problem upon satisfying some relations and requirements for a_I, $h(\phi)$, $h_{\rm inv}(\phi)$, $f_{ac}(\phi)$, and $f_{\tau,ij}(\phi)$ as described in detail in the next section. The previous nonvariational models contain a solvability integral that must be calculated in accordance with changes in the solid diffusivity and the partition coefficient during the solidification processes. As discussed later, the present form is more convenient because one can avoid introducing such an integral.

Note that the transport coefficients $M_{p,ij}$ are employed in Eqs. (63), (65), and (67); they can be replaced by $D_{p,ij}$ using the relation $M_{p,ij} = -\Sigma_k\chi^{-1}_{p,ik}D_{p,kj}$. The diffusivity is more convenient than the transport coefficient as the input parameter in terms of the availability of the measured and/or calculated values.

III. THIN-INTERFACE LIMIT ANALYSIS

We perform the asymptotic analysis of the present model [Eqs. (62) and (66)] to investigate the behavior of the solution for small W. For the sake of convenience, the spatial and time scales are normalized in terms of d_0 and $d_0^2/D_{l,0}$, where $D_{l,0}$ is a reference value of the diffusivity, which can be given by $D_{l,ii}$ with an arbitrary chosen solute atom i at a temperature. Equation (62) is rewritten in the normalized scale as follows:

$$\left(\alpha_0 + \varepsilon \sum_{i,j} \alpha_{ij} \Delta C_i M_{c,ij}^{-1} \Delta C_j\right) \varepsilon^2 \partial_t \phi = \varepsilon^2 \nabla^2 \phi - f'_{dw} - \varepsilon a_1 \tilde{g}' \frac{\Delta G_{\text{driv}}}{\chi_e} - \varepsilon^2 \sum_i a_{c,i} \nabla c_{l,i} \frac{\nabla \phi}{|\nabla \phi|}, \tag{68}$$

where

$$\alpha_0 = I D_{l,0} \frac{1}{W d_0} \frac{T_0}{\chi_e} \frac{1}{M_\phi} \tag{69}$$

and

$$\alpha_{ij} = a_I D_{l,0} \frac{T_0}{\chi_e} \frac{1-h^2}{8 f_{dw}} f_{\tau,ij}(\phi). \tag{70}$$

Also, the diffusion equation is given as

$$\frac{1+h}{2} \sum_j k_{ij}^c \partial_t c_{l,j} + \frac{1-h}{2} \partial_t c_{l,i} = \nabla \left(\sum_j \mathbf{q}_{ij} \nabla c_{l,j} + a_{AT,i}\, \varepsilon\, \partial_t \phi \frac{\nabla \phi}{|\nabla \phi|} \right) + \Delta C_i \frac{h'}{2} \partial_t \phi, \tag{71}$$

where $\mathbf{q}_{ij} = \mathbf{D}_{ij}/D_{l,0}$. Note that $\mathbf{q}_{ij} = q_{ij}(\phi = -1) = D_{l,ij}/D_{l,0}$ for $\phi = -1$ and $\mathbf{q}_{ij} = q_{ij}(\phi = +1) = \Sigma_k D_{s,ik} k_{kj}^c / D_{l,0}$ for $\phi = +1$.

The solutions of Eqs. (68) and (71) are analyzed in a perturbative manner by expanding them in inner and outer regions in powers of ε in the same manner as in Refs. [14,24,27,31]. The inner region is the interface region, while the outer region is the bulk region away from the interface. ϕ rapidly varies in the inner region and takes a constant value (+1 or −1) in the outer region. Equations (68) and (71) are rewritten using a local orthogonal set of curvilinear coordinates, the signed distance to the $\phi = 0$ level set r, and the arc length along the interface s. In the inner region, moreover, the length scale is rescaled as $\eta = r/\varepsilon$. Then, the time evolution equation of ϕ is given as

$$\partial_\eta^2 \phi - f'_{dw} + \varepsilon(\alpha_0 v_n + \kappa)\partial_\eta \phi - \varepsilon a_1 \tilde{g}' \frac{\Delta G_{\text{driv}}}{\chi_e} + \varepsilon \sum_i a_{c,i} \partial_\eta c_{l,i} - \varepsilon^2 \kappa^2 \eta \partial_\eta \phi + \varepsilon^2 \partial_s^2 \phi + \varepsilon^2 v_n \sum_{i,j} \alpha_{ij} \Delta C_i M_{c,ij}^{-1} \Delta C_j \partial_\eta \phi = 0, \tag{72}$$

where v_n and κ are the normal interface velocity and the curvature in the dimensionless scale, respectively. Equation (71) is given as

$$\varepsilon^{-2} \partial_\eta \left(\sum_j q_{ij}^n \partial_\eta c_{l,j} \right) + \varepsilon^{-1} \kappa \sum_j q_{ij}^n \partial_\eta c_{l,j} - \varepsilon^{-1} v_n \Delta C_i \frac{h'}{2} \partial_\eta \phi + \varepsilon^{-1} v_n \partial_\eta (a_{AT,i}\, \partial_\eta \phi) + \varepsilon^{-1} v_n \frac{1+h}{2} \sum_j k_{ij}^c \partial_\eta c_{l,j} + \varepsilon^{-1} v_n \frac{1-h}{2} \partial_\eta c_{l,i} - \kappa^2 \eta \sum_j q_{ij}^n \partial_\eta c_{l,j} + \partial_s \left(\sum_j q_{ij}^t \partial_s c_{l,j} \right) + \kappa v_n a_{AT,i}\, \partial_\eta \phi = 0, \tag{73}$$

where $q_{ij}^n = -\sum_k M_{n,ik} \chi_{l,kj}/D_{l,0}$ and $q_{ij}^t = -\sum_k M_{t,ik} \chi_{l,kj}/D_{l,0}$ and therefore $q_{ij}^n(\phi = \pm 1) = q_{ij}^t(\phi = \pm 1) = q_{ij}(\phi = \pm 1)$. The inner expansions of ϕ and c_i are represented by $\phi = \phi_0 + \varepsilon \phi_1 + \varepsilon^2 \phi_2 + \cdots$ and $c_{l,i} = c_{l,i,0} + \varepsilon c_{l,i,1} + \varepsilon^2 c_{l,i,2} + \cdots$, respectively, while the outer expansions are represented by $\Phi = \Phi_0 + \varepsilon \Phi_1 + \varepsilon^2 \Phi_2 + \cdots$ and $C_{l,i} = C_{l,i,0} + \varepsilon C_{l,i,1} + \varepsilon^2 C_{l,i,2} + \cdots$. The expansions in the inner region are substituted into Eqs. (72) and (73) and they are matched order by order in powers of ε to those in the outer region. The matching conditions are the same as those reported in Ref. [14]. The asymptotic analysis for the present model is carried out in the same way as in our previous work [31]. However, several important relations must be taken into account for the present case, especially regarding the diffusion matrix and the thermodynamic factor. Hence, details of the analysis are explained in Appendix B and only the essential points are described below.

Equation (72) at order ε^0 yields $\phi_0(\eta) = -\tanh(\eta/\sqrt{2})$ and $\partial_\eta \phi_0 = (\phi_0^2 - 1)/\sqrt{2}$ with the boundary conditions $\phi_0 \to -1$ for $\eta \to +\infty$ and $\phi_0 \to +1$ for $\eta \to -\infty$. One obtains $\sum_j q_{ij}^n \partial_\eta c_{l,j,0} = 0$ from Eq. (73) at order ε^{-2}. This equation must be satisfied for the regular matrix q_{ij}^n. Hence, $\partial_\eta c_{l,j,0} = 0$ and $c_{l,j,0} = C_{l,j,0}(s)$. Equation (72) at order ε yields

$$\frac{\Delta G_{\text{driv}}(\{C_{i,0}\})}{\chi_e} = -\alpha_0 v_n - \kappa. \tag{74}$$

This equation represents the Gibbs-Thomson relation at the lowest order. These solutions can be found in the same manner as in Refs. [14,24,27,31]. Next, from Eq. (73) at order ε^{-1}, one obtains

$$v_n \Delta C_i(\{C_{i,0}\}) = \sum_j q_{ij}(+1) \partial_r C_{l,j,0}|^- - \sum_j q_{ij}(-1) \partial_r C_{l,j,0}|^+, \tag{75}$$

where $A|^+$ and $A|^-$ represent the values of A on the liquid and solid sides of the interface, respectively. Equation (75) represents the Stefan condition at the lowest order. In addition,

the following relation is obtained:

$$-\frac{1}{D_{l,0}}\sum_j \chi_{l,ij} C_{l,j,1}|^{\pm} = \frac{1}{2}v_n \sum_j M^{-1}_{l,ij}\Delta C_j H^{\pm} + \sum_{j,k} G^{\pm}_{ij} q_{jk}(+1)\partial_r C_{l,k,0}|^{-} + A_{i,0}, \tag{76}$$

where $A_{i,0}$ is the integral constant and

$$H^{\pm} = \int_0^{\pm\infty} (h \pm 1) d\xi, \tag{77}$$

$$G^{\pm}_{ij} = \int_0^{\pm\infty} \left[M^{-1}_{n,ij}(\phi_0) - M^{-1}_{n,ij}(\mp 1)\right] d\xi = \frac{\left(M^{-1}_{s,ij} - M^{-1}_{l,ij}\right)}{2}\int_0^{\pm\infty} (h_{\rm inv} \pm 1) d\xi. \tag{78}$$

Therefore, $H^+ = H^-$ and $G^+_{ij} = G^-_{ij}$ are required for the diffusion potential to be continuous across the diffuse interface. This requirement is automatically satisfied in the variational model because $h = h_{\rm inv} = g$. Furthermore, this requirement can be satisfied when h and $h_{\rm inv}$ are an odd function of ϕ. Details of the analysis of Eq. (73) at order ε^{-1} are explained in Appendix B.

The integral constant $A_{i,0}$ in Eq. (76) can be obtained from Eq. (72) at order ε^2, and one can derive the following relation:

$$\sum_i \frac{\partial \Delta G_{\rm driv}}{\partial c_{l,i}} C_{l,i,1}|^{\pm} = v_n T_0 D_{l,0}\left\{\sum_{i,j} \Delta C_i M^{-1}_{l,ij}\Delta C_j (a_1 a_2 + a_{3,ij})\right\}. \tag{79}$$

where $a_1 = I/J$ and

$$a_2 = \frac{JH^{\pm} + K}{2I}, \tag{80}$$

$$a_{3,ij} = \frac{a_I}{I}\int_{-\infty}^{+\infty}\left[\frac{M^{-1}_{c,ij}}{M^{-1}_{l,ij}}[f_{ac}(\phi) - f_{\tau,ij}(\phi)] - f_{ac}(\phi)\right] \times \frac{1-h^2}{4} d\xi \tag{81}$$

with

$$K = \int_{-\infty}^{+\infty}\left(\int_0^{\eta} h d\xi\right)\tilde{g}'(\phi_0)\partial_\eta \phi_0 d\xi. \tag{82}$$

For Eq. (79) to be valid, a_I must satisfy

$$a_I = I\left(\int_{-\infty}^{+\infty}(1 - h_{\rm inv} g) d\xi\right)\Big/ \int_{-\infty}^{+\infty} f_{ac}(\phi)(1 - h_{\rm inv})(1 + h) d\xi. \tag{83}$$

In the variational model, Eq. (83) always holds because $h = h_{\rm inv} = g$, $f_{ac}(\phi) = 1$ and $a_I = I$. In the nonvariational model, a_I must be determined based on Eq. (83) to remove a constant error in the Gibbs-Thomson relation which appears not in one-sided diffusion but in two-sided asymmetric diffusion. In addition, in deriving Eq. (79), we employed the following relation for the thermodynamic quantities:

$$\sum_i \frac{\partial \Delta G_{\rm driv}}{\partial c_i}\chi^{-1}_{l,ij} = -T_0 \Delta C_j, \tag{84}$$

which can be obtained from Eq. (39). More details are explained in Appendix B. By combining Eqs. (74) and (79), one obtains

$$\frac{\Delta G_{\rm driv}(\{X_{i,0}\})}{\chi_e} + \varepsilon \sum_i \frac{1}{\chi_e}\frac{\partial \Delta G_{\rm driv}}{\partial c_{l,i}} C_{l,i,1}|^{\pm} = -\beta v_n - \kappa, \tag{85}$$

where

$$\beta = \alpha_0 - \varepsilon T_0 \frac{D_{l,0}}{\chi_e}\left\{\sum_{i,j}\Delta C_i M^{-1}_{l,ij}\Delta C_j (a_1 a_2 + a_{3,ij})\right\}. \tag{86}$$

Equation (85) is equivalent to the Gibbs-Thomson relation described by Eq. (60) with $\beta = D_{l,0}/(\gamma\,\mu_{\rm int})$. It is important to point out that in the variational model, $a_{3,ij}$ is calculated to be $-a_1 a_2$ and the second term on the right-hand side of Eq. (86) vanishes, which results in $\beta = \alpha_0$. Namely, the phase-field mobility M_ϕ is exactly proportional to the interface mobility $\mu_{\rm int}$. This is in contrast to the conventional quantitative models, where the phase-field mobility depends on $\{c_{l,i}\}$ even though $\mu_{\rm int}$ is assumed to be a constant [14,24]. This fact was not explicitly discussed in the previous study [31].

One can obtain the following relation from Eq. (73) at order ε^0:

$$v_n\left(C_{l,i,1}|^{+} - \sum_j k^c_{ij} C_{l,j,1}|^{-}\right) = \sum_j q_{ij}(+1)\partial_r C_{l,j,1}|^{-} + \sum_{j,k}\frac{\partial q_{ij}(+1)}{\partial c_k} C_{l,k,1}|^{-}\partial_r C_{l,j,0}|^{-} - \sum_j q_{ij}(-1)\partial_r C_{l,j,1}|^{+} - \sum_{j,k}\frac{\partial q_{ij}(-1)}{\partial c_k} C_{l,k,1}|^{+}\partial_r C_{l,j,0}|^{+}. \tag{87}$$

This relation is valid as long as the following requirements are satisfied:

$$\int_0^{-\infty}\left[q^t_{ij} - q_{ij}(+1)\right] d\xi = \int_0^{+\infty}\left[q^t_{ij} - q_{ij}(-1)\right] d\xi, \tag{88}$$

$$\frac{\partial}{\partial c_{l,k}}\int_0^{-\infty}\left[q^t_{ij} - q_{ij}(+1)\right] d\xi = \frac{\partial}{\partial c_{l,k}}\int_0^{+\infty}\left[q^t_{ij} - q_{ij}(-1)\right] d\xi, \tag{89}$$

that are related to the correction associated with surface diffusion. According to Eq. (48), when g is replaced by h, Eqs. (88) and (89) are equivalent to the requirement of

$H^+ = H^-$. Hence, Eqs. (88) and (89) are satisfied in both the variational and nonvariational models. One finally obtains the following relation from Eqs. (75) and (87):

$$\begin{aligned} v_n &\left(\Delta C_i + \varepsilon C_{l,i,1}\big|^+ - \varepsilon \sum_j k_{ij}^c C_{l,j,1}\big|^- \right) \\ &= \sum_j q_{ij}(+1)\,\partial_r C_{l,j,0}\big|^- - \sum_j q_{ij}(-1)\,\partial_r C_{l,j,0}\big|^+ \\ &\quad + \varepsilon \sum_j q_{ij}(+1)\,\partial_r C_{l,j,1}\big|^- - \varepsilon \sum_j q_{ij}(-1)\,\partial_r C_{l,j,1}\big|^+ \\ &\quad + \varepsilon \sum_{j,k} \frac{\partial q_{ij}(+1)}{\partial c_{l,k}} C_{l,k,1}|^- \partial_r C_{l,j,0}|^- \\ &\quad - \varepsilon \sum_{j,k} \frac{\partial q_{ij}(-1)}{\partial c_{l,k}} C_{l,k,1}\big|^+ \partial_r C_{l,j,0}\big|^+. \end{aligned} \tag{90}$$

This equation is equivalent to the Stefan condition given by Eq. (61).

As demonstrated above, the variational phase-field model developed in this study exactly reproduces the sharp-interface equations (59)–(61) without any modification in the thin-interface limit. This fact demonstrates the validity and usefulness of the present variational formulation. In the case of a nonvariational model, furthermore, the sharp-interface equations can be reproduced as long as $H^+ = H^-$ and $G_{ij}^+ = G_{ij}^-$ are satisfied, a_I is given by Eq. (83), and a_0 (hence, the phase-field mobility M_ϕ) is given by Eq. (86).

IV. SPECIFIC EXAMPLES FOR SOME SYSTEMS

A. Definition of functions in nonvariational model

Equations (62) and (66) represent the general form of the present model. This model can be applied to a variety of solidification problems and also diffusion-controlled solid-solid transformations. It should be helpful for further understanding of the present model and its practical use to illustrate specific forms of the model for well-known problems. In this section, specific forms are demonstrated for solidification in a pure substance, isothermal solidification in a binary alloy and also nonisothermal solidification in a multicomponent alloy with an approximated driving force. In particular, the nonvariational forms are discussed. Before going into the details of each case, we explain the forms of $h(\phi)$, $h_{\rm inv}(\phi)$, $f_{ac}(\phi)$, and $f_{\tau,ij}(\phi)$ that are employed in all these models.

As described in Sec. II E, the model derived in a variational manner does not necessarily exhibit high numerical performance, i.e., fast convergence of the results with decreasing W [12,31]. Our preliminary simulations showed that the convergence of the present variational model is also slow. This is because of two reasons. The first reason is related to $h(\phi)$ which interpolates c_i inside the interface. $h(\phi)$ of a high-order polynomial causes rapid variation of c_i near the center of the interface and description of such rapid variation requires a small spatial grid spacing as discussed in Ref. [40]. To avoid this problem, in this study, $h(\phi)$ is defined as $h(\phi) = \phi$, which generally yields good numerical performance [12,40]. The second reason for slow convergence in the variational model originates from $M_{n,ij}$ [Eq. (51)] where the inverse of the transport coefficient (or diffusivity) in each bulk is interpolated inside the interface, which is called inverse interpolation in this paper. In the variational model where $h_{\rm inv}(\phi) = g(\phi)$, $M_{n,ij}$ sharply changes inside the interface when the difference in the transport coefficient (diffusivity) between the solid and liquid is large. This is numerically unfavorable [31]. In nonvariational models, a form of $h_{\rm inv}(\phi)$ can be chosen so as to prevent this problem. In this section, $h_{\rm inv}(\phi)$ is given as $h_{\rm inv}(\phi) = \phi$ because this choice makes it possible to illustrate specific forms of the model in a concise way. Also, preliminary simulations showed that this choice yields reasonable numerical performance in some cases where differences in diffusivity between the solid and liquid are not very large. In the next section, we propose a different form of $h_{\rm inv}(\phi)$ to achieve much better numerical performance.

In defining $f_{ac}(\phi)$, one must pay attention to the requirement that the cross-coupling term in the ϕ equation must vanish outside the interface. Note that the right-hand side of Eq. (62) must vanish outside the interface because ϕ should take constant values of $+1$ in the bulk solid and -1 in the bulk liquid. In the variational model, this is automatically satisfied because $a_{c,i}$ in Eq. (63) becomes zero at $\phi = \pm 1$. It can be readily confirmed by noting $h = h_{\rm inv} = g$ and $(f_{dw})^{1/2} = (1-\phi^2)/2$. However, $a_{c,i}$ does not automatically vanish at $\phi = \pm 1$ when $h = h_{\rm inv} = \phi$ is employed in the nonvariational model. Hence, f_{ac} needs to be defined so as to satisfy the condition of $a_{c,i} = 0$ at $\phi = \pm 1$. There are several possible forms for $f_{ac}(\phi)$. In this study, $f_{ac}(\phi)$ is given as

$$f_{ac}(\phi) = 2(1-\phi^2). \tag{91}$$

Then, a_I can be calculated from Eq. (83) as

$$a_I = 2a_1a_2 I \Big/ \int_{-\infty}^{+\infty} (1-\phi^2)^2 d\xi = a_1 a_2, \tag{92}$$

where $a_1 = 5\sqrt{2}/8$ and $a_2 = 0.6267$. For $f_{\tau,ij}(\phi)$, we employ the following form:

$$f_{\tau,ij}(\phi) = f_{ac}(\phi)\left(1 - \frac{M_{l,ij}^{-1}}{M_{c,ij}^{-1}}\right), \tag{93}$$

which results in $a_{3,ij} = 0$. Therefore, M_ϕ can be obtained from Eq. (86) as follows:

$$\frac{1}{M_\phi} = \frac{W}{IT_0}\frac{1}{\mu_{\rm int}} + \frac{W^2}{I}\left\{\sum_{i,j} \Delta C_i M_{l,ij}^{-1} \Delta C_j\right\} a_1 a_2. \tag{94}$$

By substituting Eqs. (92)–(94) into Eq. (65), one obtains

$$\tau = \frac{W^2}{d_0\chi_e}\frac{1}{\mu_{\rm int}} + a_1 a_2 \frac{W^3}{d_0}\frac{T_0}{\chi_e}\sum_{i,j} \Delta C_i M_{c,ij}^{-1} \Delta C_j. \tag{95}$$

In our previous nonvariational models for isothermal solidification [31], the solvability integral included in the expression for τ depends on the solid diffusivity and the partition coefficient. Hence, one must calculate the change in the integral during the solidification process unless the solid diffusivity and partition coefficient are assumed constant. On the other hand, the present nonvariational model does not

include such an integral and it is more convenient for numerical implementation than the previous models.

It is important to point out that the entropy is the thermodynamic potential in the present formulation and therefore the thermodynamic quantities such as $\Delta G_{\rm driv}$ and $\chi_{p,ij}$ in this model are functions of the energy density and the compositions. This point should be taken into account when approximations and simplifications are introduced into the present model. In particular, care must be paid to the thermodynamic relation given by Eq. (84), which must be satisfied to ensure the consistency of the model with the free-boundary problem. As long as these points are appropriately taken into account when applying the present model to specific cases, the set of independent variables can be changed to a set of different variables. For instance, the energy density e_l can be changed to the temperature field T when the temperature dependence of e_l is defined as shown below.

B. Solidification in a pure substance

We first focus on the solidification in a pure substance. In this case, the independent variables are ϕ and e_l. However, it is convenient for the description of the heat conduction problem to use the temperature instead of the energy. Therefore, we choose the temperature field T as the independent variable by using a relation $e_l = e_l(T)$. Equations (62) and (66) can be rewritten as

$$\tau\,\partial_t\phi = W^2\nabla^2\phi - f'_{dw} - \widetilde{g}'a_1\frac{W}{d_0}\frac{\Delta G_{\rm driv}}{\chi_e} - \frac{W^2}{d_0}a_c\nabla T\cdot\frac{\nabla\phi}{|\nabla\phi|}, \tag{96}$$

$$\left(\frac{1+\phi}{2}C_{s,V} + \frac{1-\phi}{2}C_{l,V}\right)\partial_t T = \nabla\cdot\left(\lambda_T\nabla T + a_{AT}W\partial_t\phi\frac{\nabla\phi}{|\nabla\phi|}\right) + \frac{\Delta L}{2}\partial_t\phi, \tag{97}$$

where $\Delta G_{\rm driv} = f_{s,\rm bulk}(T) - f_{l,\rm bulk}(T)$, $C_{l,V} = de_l/dT$, $C_{s,V} = de_s/dT = k^c C_{l,V}$ with $k^c = de_s/de_l = (d^2s_l/de_l^2)/(d^2s_s/de_s^2)$, and $\Delta L = e_l - e_s$. $C_{l,V}$ and $C_{s,V}$ are the specific heat per unit volume in the liquid and solid, respectively and ΔL is the latent heat per unit volume. Also,

$$\tau = \frac{W^2}{d_0\chi_e}\frac{1}{\mu_{\rm int}} + a_1a_2\frac{W^3}{d_0}\frac{2\Delta L}{\lambda_{s,T}(1-\phi)+\lambda_{l,T}(1+\phi)}\times\frac{1}{\chi_e}\frac{d\Delta G_{\rm driv}}{dT}, \tag{98}$$

$$a_c = -\sqrt{2}a_1a_2(1-\phi^2)\frac{(\lambda_{l,T}-\lambda_{s,T})}{\lambda_{s,T}(1-\phi)+\lambda_{l,T}(1+\phi)}\times\frac{1}{\chi_e}\frac{d\Delta G_{\rm driv}}{dT}, \tag{99}$$

$$a_{AT} = \frac{1}{\sqrt{2}}\frac{(\lambda_{l,T}-\lambda_{s,T})}{(1-\phi)\lambda_{s,T}+(1+\phi)\lambda_{l,T}}\Delta L, \tag{100}$$

$$\lambda_T = \frac{2\lambda_{s,T}\lambda_{l,T}}{(1-\phi)\lambda_{s,T}+(1+\phi)\lambda_{l,T}}\mathbf{n}\otimes\mathbf{n} + \left(\frac{1+\phi}{2}\lambda_{s,T} + \frac{1-\phi}{2}\lambda_{l,T}\right)(\mathbf{1}-\mathbf{n}\otimes\mathbf{n}), \tag{101}$$

where $\lambda_{p,T}$ is the thermal conductivity of phase p given as $\lambda_{p,T} = D_{p,T}C_{p,V}$ with thermal diffusivity $D_{p,T} = -M_{p,T}(d^2s_p/de_p^2)$. In deriving Eqs. (98) and (99), $\chi_{l,ee} = d^2s_p/d(\Omega e_p)^2$ was calculated using Eq. (84). This model can reproduce the solution of the following free-boundary problem:

$$C_{p,V}\partial_t T = \nabla\cdot(\lambda_{p,T}\nabla T) \text{ in phase } p, \tag{102}$$

$$f_{s,\rm bulk} - f_{l,\rm bulk} = -\frac{1}{\mu_{\rm int}}V_n - \gamma\kappa, \tag{103}$$

$$\Delta L V_n = \lambda_{s,T}\partial_r T|^- - \lambda_{l,T}\partial_r T|^+. \tag{104}$$

Here, one can utilize, for instance, the free energy function of the SGTE database [41] for $f_{p,\rm bulk}$. When $\lambda_{l,T} = \lambda_{s,T}$ is considered, the present model becomes very tractable in numerical implementation because the cross-coupling terms between ϕ and T (a_c and a_{AT} terms) vanish and $\boldsymbol{\lambda}_T$ in Eq. (101) becomes scalar ($\boldsymbol{\lambda}_T = \lambda_{l,T}$). Also, the early model for a pure substance [12] can be reproduced by introducing the following simplifications and approximations: $\Delta G_{\rm driv} = f_{s,\rm bulk}(T) - f_{l,\rm bulk}(T) \approx (\Delta L/T_m)(T - T_m)$, $\Delta L =$ const, $C_{l,V} = C_{s,V} =$ const, $\lambda_{l,T} = \lambda_{s,T} =$ const, and $\chi_e = \Delta L^2/(T_m C_{l,V})$, with which d_0 becomes the thermal capillary length.

C. Isothermal solidification in a binary alloy

In the case of isothermal solidification in a binary alloy, the independent variables are ϕ and c_l. The interface temperature T_0 corresponds to the holding temperature. Then, the time evolution equations of ϕ and c_l are given as

$$\tau\,\partial_t\phi = W^2\nabla^2\phi - f'_{dw} - \widetilde{g}'a_1\frac{W}{d_0}\frac{\Delta G_{\rm driv}}{\chi_e} - \frac{W^2}{d_0}a_c\nabla c_l\cdot\frac{\nabla\phi}{|\nabla\phi|}, \tag{105}$$

$$\left(\frac{1+\phi}{2}k^c + \frac{1-\phi}{2}\right)\partial_t c_l = \nabla\cdot\left(\mathbf{D}\nabla c_l + a_{AT}W\partial_t\phi\frac{\nabla\phi}{|\nabla\phi|}\right) + \frac{(c_l-c_s)}{2}\partial_t\phi, \tag{106}$$

where

$$\tau = \frac{W^2}{d_0\chi_e}\frac{1}{\mu_{\rm int}} + a_1a_2\frac{W^3}{d_0}\frac{2(c_l-c_s)^2}{(1-\phi)k^cD_s+(1-\phi)D_l}\times\frac{1}{\chi_e}\frac{\partial\Delta\mu_c}{\partial c_l}, \tag{107}$$

$$\Delta G_{\rm driv} = f_{s,\rm bulk} - f_{l,\rm bulk} - \Delta\mu_c(c_s - c_l), \tag{108}$$

$$a_c = -\sqrt{2}a_1a_2(1-\phi^2)(c_l-c_s)\frac{D_l-k^cD_s}{(1-\phi)k^cD_s+(1-\phi)D_l}\times\frac{1}{\chi_e}\frac{\partial\Delta\mu_c}{\partial c_l}, \tag{109}$$

$$a_{AT} = \frac{1}{\sqrt{2}}(c_l-c_s)\frac{D_l-k^cD_s}{k^cD_s(1-\phi)+D_l(1-\phi)}, \tag{110}$$

$$\mathbf{D} = \frac{2k^c D_s D_l}{(1-\phi)k^c D_s + (1+\phi)D_l}\mathbf{n}\otimes\mathbf{n} + \left(\frac{1+\phi}{2}k^c D_s + \frac{1-\phi}{2}D_l\right)(\mathbf{1}-\mathbf{n}\otimes\mathbf{n}), \quad (111)$$

where $k^c = dc_s/dc_l = (d^2s_l/dc_l^2)/(d^2s_s/dc_s^2)$, $D_l = -M_l(d^2s_l/dc_l^2)$, and $k^c D_s = -M_s(d^2s_l/dc_l^2) = -k^c M_s(d^2s_s/dc_s^2)$. d_0 is the chemical capillary length when χ_e is defined as $(c_l^e - c_s^e)^2\,\partial\Delta\mu_l/\partial c_l|_e$, where c_p^e is the equilibrium composition of phase p and $A|_e$ represents the value of A at equilibrium. This model is consistent with the following free-boundary problem:

$$\partial_t c = \nabla\cdot(D_p\nabla c) \text{ in phase } p, \quad (112)$$

$$f_{s,\text{bulk}} - f_{l,\text{bulk}} - \Delta\mu_c(c_s^* - c_l^*) = -\frac{1}{\mu_{\text{int}}}V_n - \gamma\kappa, \quad (113)$$

$$(c_l^* - c_s^*)\,V_n = D_s\,\partial_r c|^- - D_l\partial_r c|^+, \quad (114)$$

where c_l^* and c_s^* are the compositions at the interface in the liquid and solid, respectively, at the interface. Note that one can utilize any type of free energy model for $f_{p,\text{bulk}}$, such as the solution model in the CALPHAD method [38], and one can consider the concentration dependence of the diffusivities.

Let us remark on a numerical issue in this model. Except for a case that a simplified model such as a dilute solution model is employed for bulk's free energy density, c_s must be calculated at each spatial point such that the condition of equal diffusion potentials [Eq. (35)] is satisfied. Although this can be carried out by an iterative calculation method such as the Newton-Raphson method, it is often time consuming. On the other hand, instead of conducting such an iterative calculation, one can directly calculate the temporal change in c_s from $\partial_t c_s = k^c\partial_t c_l$ with $\partial_t c_l$ and k^c obtained from c_l and c_s at t. The calculated c_s satisfies Eq. (35) as long as the initial value of c_s satisfies Eq. (35).

D. Nonisothermal solidification in a multicomponent alloy: Linearized driving force

A simplified model for nonisothermal solidification in a multicomponent alloy with n solute atoms is next demonstrated. The independent variables are chosen to be T and $c_{l,i}$ with $i \leqslant n$. The contributions of off-diagonal diffusivities are neglected for simplicity. In addition, we employ the approximation called the multibinary extrapolation [42] for the driving force. The following form of the driving force is assumed:

$$\Delta G_{\text{driv}} = \Delta S_{\text{driv}}(T - T_0) + \Delta S_{\text{driv}}\sum_i m_{l,i}\left(c_{l,i} - c_{l,i}^0\right), \quad (115)$$

where ΔS_{driv} is the entropy contribution of the driving force and $m_{l,i}$ is the liquidus slope of solute i, which are both approximated as constants. $c_{l,i}^0$ is the equilibrium composition of i at the liquidus temperature T_0. Also, $\chi_{l,ij} = 0$ is assumed for $i \neq j$. Then, from Eq. (84), the second derivative of the entropy density is expressed as

$$\chi_{l,ee} = \frac{\partial^2 s_{l,\text{bulk}}}{\Omega^2\partial e_l^2} = -\frac{1}{\Omega^2 T_0\Delta L}\frac{\partial\Delta G_{\text{driv}}}{\partial T}\frac{\partial T}{\partial e_l} = -\frac{\Delta S_{\text{driv}}}{\Omega^2 T_0\Delta L}\frac{1}{C_V} \quad (116)$$

for the energy density and

$$\chi_{l,ii} = \frac{\partial^2 s_{l,\text{bulk}}}{\partial c_{l,i}^2} = -\frac{1}{T_0\Delta C_i}\frac{\partial\Delta G_{\text{driv}}}{\partial c_i} = -\frac{\Delta S_{\text{driv}} m_{l,i}}{T_0\Delta C_i} \quad (117)$$

for solute i. In these expressions, $\partial e_l/\partial c_{l,i}$ is assumed to be negligible and $\partial e_l/\partial T$ is set to C_V, which is the constant specific heat with $C_{l,V} = C_{s,V} = C_V$. Then, the ϕ equation is given as

$$\tau\,\partial_t\phi = W^2\nabla^2\phi - f'_{dw} - \widetilde{g}' a_1\frac{W}{d_0}\frac{\Delta G_{\text{driv}}}{\chi_e} - \frac{W^2}{d_0}\left(a_{c,T}\nabla T + \sum_{i=1}^n a_{c,i}\nabla c_{l,i}\right)\cdot\frac{\nabla\phi}{|\nabla\phi|}, \quad (118)$$

$$\tau = \frac{W^2}{d_0\chi_e}\frac{1}{\mu_{\text{int}}} + 2a_1a_2\frac{W^3}{d_0}\frac{\Delta S_{\text{driv}}}{\chi_e}\left(\frac{\Delta L/C_V}{(1-\phi)D_{s,T} + (1+\phi)D_{l,T}} + \sum_{i=1}^n\frac{(c_{l,i} - c_{s,i})m_{l,i}}{(1-\phi)k_i^c D_{s,i} + (1+\phi)D_{l,i}}\right), \quad (119)$$

$$a_{c,T} = -\sqrt{2}a_1a_2(1-\phi^2)\frac{D_{l,T} - D_{s,T}}{(1-\phi)D_{s,T} + (1+\phi)D_{l,T}}\frac{\Delta S_{\text{driv}}}{\chi_e}, \quad (120)$$

$$a_{c,i} = -\sqrt{2}a_1a_2(1-\phi^2)\frac{D_{l,i} - k_i^c D_{s,i}}{(1-\phi)k_i^c D_{s,i} + (1+\phi)D_{l,i}}\frac{\Delta S_{\text{driv}} m_{l,i}}{\chi_e}, \quad (121)$$

where $D_{p,T}$ and $D_{p,i}$ are the thermal diffusivity and diffusivity of solute i in phase p, respectively, and $k_i^c = m_{l,i}/m_{s,i}$ with $m_{s,i}$ the solidus slope of solute i. The time evolution of the temperature is described by

$$\partial_t T = \nabla\cdot\left(\mathbf{D}_T\nabla T + a_{AT,T}W\partial_t\phi\frac{\nabla\phi}{|\nabla\phi|}\right) + \frac{\Delta L}{C_V}\frac{\partial_t\phi}{2}, \quad (122)$$

with

$$a_{AT,T} = \frac{1}{\sqrt{2}}\frac{(D_{l,T} - D_{s,T})}{(1-\phi)D_{s,T} + (1+\phi)D_{l,T}}\frac{\Delta L}{C_V}, \quad (123)$$

where $\mathbf{D}_T$ is given by Eq. (111) with $k^c D_s$ and D_l replaced by $D_{s,T}$ and $D_{l,T}$, respectively. The diffusion equation of solute i is given as

$$\left(\frac{1+\phi}{2}k_i^c + \frac{1-\phi}{2}\right)\partial_t c_i = \nabla\cdot\left(\mathbf{D}_i\nabla c_i + a_{AT,i}W\partial_t\phi\frac{\nabla\phi}{|\nabla\phi|}\right) + (c_{l,i} - c_{s,i})\frac{\partial_t\phi}{2}, \quad (124)$$

with

$$a_{AT,i} = \frac{1}{\sqrt{2}}(c_{l,i} - c_{s,i})\frac{D_{l,i} - k_i^c D_{s,i}}{(1-\phi)k_i^c D_{s,i} + (1+\phi)D_{l,i}}, \quad (125)$$

where $\mathbf{D}_i$ is given as Eq. (111) with $k^c D_s$ and D_l replaced by $k_i^c D_{s,i}$ and $D_{l,i}$, respectively.

V. NUMERICAL TEST

Numerical testing was carried out to evaluate the performance of the present nonvariational model. The convergence behavior of the simulation result was investigated by decreasing the interface thickness W in a similar manner as in the previous studies [14,24,27,31,40]. We performed two-dimensional simulations of dendritic growth during nonisothermal solidification in a ternary alloy using the model described in Sec. IV D. The independent variables are ϕ, T, $c_{l,1}$, and $c_{l,2}$. For simplicity, we assumed $1/\mu_{\rm int} = 0$, $C_V = \text{const}$, and $\Delta L = \text{const}$. Also, the partition coefficients k_i^c, the thermal diffusivities of the solid $D_{s,T}$ and liquid $D_{l,T}$, and the solute diffusivities of the solid $D_{s,i}$ and liquid $D_{l,i}$ were assumed constant. A test with these simplifications is sufficient for the present purpose. χ_e is given as $\chi_e = \Delta S_{\rm driv}(\Delta L/C_V)$ and then d_0 corresponds to the thermal capillary length.

As described in Sec. IV A, a model with $h(\phi) = \phi$ generally yields good numerical performance [12,40] and hence we employ $h(\phi) = \phi$ in this test. Although the model with $h_{\rm inv}(\phi) = \phi$ was presented for illustrative purpose in Sec. IV, we put forward a different form of $h_{\rm inv}(\phi)$ to achieve good numerical performance in this section. For clarity, the diffusivity $\mathbf{D}_i$ in Eq. (124) is described as

$$\begin{aligned}\frac{\mathbf{D}_i}{D_{l,i}} &= \frac{2q_{s,i}}{(1-h_{\rm inv})q_{s,i} + 1 + h_{\rm inv}}\mathbf{n}\otimes\mathbf{n} \\ &\quad + \left(\frac{1+\phi}{2}q_{s,i} + \frac{1-\phi}{2}\right)(\mathbf{1} - \mathbf{n}\otimes\mathbf{n}) \\ &= q_i^n\,\mathbf{n}\otimes\mathbf{n} + q_i^t\,(\mathbf{1} - \mathbf{n}\otimes\mathbf{n}), \end{aligned} \quad (126)$$

with $q_{s,i} = k_i^c D_{s,i}/D_{l,i}$ for $i = 1$, 2 and T. k_T^c is given as $k_T^c = 1.0$. q_i^n is described by inverse interpolation with $h_{\rm inv}(\phi)$, while q_i^t is given by normal interpolation with $h(\phi) = \phi$. When $q_{s,i}$ is low, q_i^n abruptly changes near $\phi = -1$ in models with $h_{\rm inv}(\phi) = g(\phi)$ or ϕ, which causes low accuracy in numerical simulations. In nonvariational models, a form of $h_{\rm inv}(\phi)$ can be chosen so as to prevent this problem. Note that $h_{\rm inv}(\phi)$ does not need to be an odd function. Any function can be employed for $h_{\rm inv}(\phi)$ as long as it satisfies $h_{\rm inv}(\pm 1) = \pm 1$ and $G_{ij}^+ = G_{ij}^-$ [Eq. (78)]. In this study, the following function is employed:

$$h_{\rm inv}(\phi) = \frac{q_a - 1 + (q_a + 1)\,h_{\rm norm}(\phi)}{q_a + 1 + (q_a - 1)\,h_{\rm norm}(\phi)}, \quad (127)$$

where q_a is a constant and $h_{\rm norm}(\phi)$ is the odd function given as

$$h_{\rm norm}(\phi) = \phi + a_4\phi(1-\phi^2), \quad (128)$$

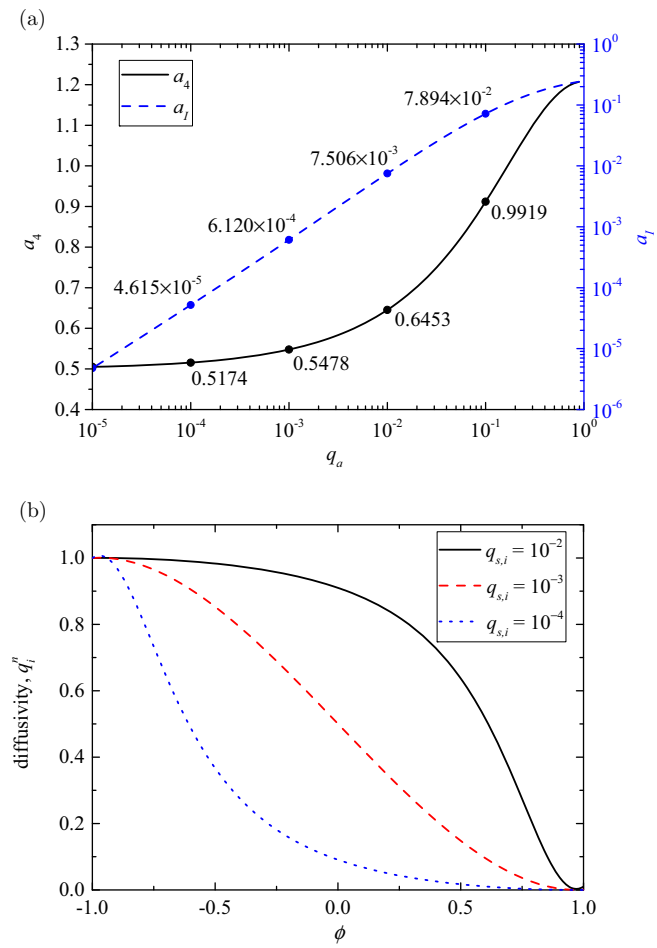

FIG. 1. (a) Dependence of a_4 and a_I on q_a. (b) Dependence of diffusivity q_i^n on ϕ calculated for $q_{s,i} = 10^{-2}$, 10^{-3}, and 10^{-4}. $q_a = 10^{-3}$ and $a_4 = 0.5478$ were employed in (b).

with a constant a_4. This function was chosen because it can be rewritten as

$$\frac{2q_a}{(1-h_{\rm inv})q_a + (1+h_{\rm inv})} = \frac{1+h_{\rm norm}}{2}q_a + \frac{1-h_{\rm norm}}{2}, \quad (129)$$

where the left-hand side represents the inverse interpolation between 1 and q_a with $h_{\rm inv}(\phi)$, while the right-hand side represents the normal interpolation between 1 and q_a with $h_{\rm norm}(\phi)$. This property of $h_{\rm inv}(\phi)$ is beneficial in suppressing an abrupt change of q_i^n associated with the inverse interpolation. The constant a_4 must be determined so as to satisfy $G_{ij}^+ = G_{ij}^-$ for each value of q_a. The calculated value of a_4 is shown in Fig. 1(a) where four values are denoted for reference. The advantage of $h_{\rm inv}(\phi)$ given by Eq. (127) is exemplified in Fig. 1(b) which shows dependence of q_i^n on ϕ calculated for $q_{s,i} = 10^{-2}$, 10^{-3}, and 10^{-4}. In these calculations, $q_a = 10^{-3}$ ($a_4 = 0.5478$) is employed as an example. q_i^n smoothly changes from $q_{s,i}$ to 1.0 in all cases. Hence, the problem with the abrupt change of q_i^n can be avoided by using $h_{\rm inv}(\phi)$ given by Eq. (127). In the present simulation, $q_a = 10^{-3}$ was chosen by considering values of $\{q_{s,i}\}$ mentioned below. Note that a_I given by Eq. (83) depends on the form

of $h_{\rm inv}(\phi)$ and thereby q_a. The calculated value of a_I for different q_a is shown in Fig. 1(a).

By considering the anisotropy of the fourfold symmetry in the interfacial energy, Eq. (118) is rewritten as

$$\tau_0\, a_s(\mathbf{n})^2\left[\sum_i \frac{M_{u,i}}{\mathrm{Le}_i}\left(1+\frac{1-q_{c,i}}{q_{c,i}}\frac{a_I}{a_1a_2}\right)\left[1+\left(1-k_i^c\right)u_i\right]\right]\partial_t\phi$$
$$=\nabla\cdot\left[W(\mathbf{n})^2\nabla\phi\right]+\partial_x\left(|\nabla\phi|^2W(\mathbf{n})\frac{\partial W(\mathbf{n})}{\partial(\partial_x\phi)}\right)+\partial_y\left(|\nabla\phi|^2W(\mathbf{n})\frac{\partial W(\mathbf{n})}{\partial(\partial_y\phi)}\right)$$
$$-f'_{dw}-\widetilde{g}'\lambda\left(\sum_i M_{u,i}u_i\right)+\frac{W(\mathbf{n})^2}{d_0}\sum_i \bar{a}_{c,i}M_{u,i}\nabla u_i\cdot\frac{\nabla\phi}{|\nabla\phi|}, \tag{130}$$

where the summation is carried out for $i=1,2$ and T. $u_T=\theta$ is the dimensionless undercooling given by

$$\theta=\frac{T-T_0}{\Delta L/C_V}, \tag{131}$$

and u_i with $i=1,2$ is the dimensionless supersaturation given by

$$u_i=\frac{c_{l,i}-c_{l,i}^0}{c_{l,i}^0\left(1-k_i^c\right)}. \tag{132}$$

Also,

$$W(\mathbf{n})=W_0a_s(\mathbf{n})=W_0\left(1-3\varepsilon_4+4\varepsilon_4\frac{(\partial_x\phi)^4+(\partial_y\phi)^4}{|\nabla\phi|^4}\right), \tag{133}$$

where $W_0=\varepsilon/\sqrt{\omega}$ and ε_4 is the anisotropic strength of the interfacial energy. In Eq. (130), Le_i with $i=1,2$ is the Lewis number of solute i given by $\mathrm{Le}_i=D_T/D_{l,i}$ and $M_{u,i}$ with $i=1,2$ is the ratio of thermal capillary length to the chemical capillary length of solute i given by $M_{u,i}=m_{l,i}(1-k_i^c)c_{l,i}^0/(\Delta L/C_V)$. Also, $\mathrm{Le}_T=1.0$, $M_{u,T}=1.0$, $k_T^c=1.0$, $\lambda=a_1W_0/d_0$, $\tau_0=a_2\lambda W_0^2/D_{l,T}$, and $q_{c,i}$ is given as

$$q_{c,i}=\frac{1-h_{\rm inv}}{2}q_{s,i}+\frac{1+h_{\rm inv}}{2}. \tag{134}$$

$\bar{a}_{c,i}$ is given as

$$\bar{a}_{c,i}=\frac{1}{2\sqrt{2}}a_I(1-\phi^2)[1-a_4\phi(1+\phi)]\frac{(1-h_{\rm inv})q_a+1+h_{\rm inv}}{q_a}\left(\frac{1-q_{s,i}}{q_{c,i}}\right). \tag{135}$$

The time evolution equation of u_i with $i=1,2$ and T ($u_T=\theta$) is given as

$$\frac{1}{2}\left[1+k_i^c-\left(1-k_i^c\right)\phi\right]\partial_tu_i=\nabla\cdot\left(\mathbf{D}_i\nabla u_i+\bar{a}_{AT,i}W_0\partial_t\phi\frac{\nabla\phi}{|\nabla\phi|}\right)+\frac{1}{2}\left[1+\left(1-k_i^c\right)u_i\right]\partial_t\phi, \tag{136}$$

where $\mathbf{D}_i$ is given by Eq. (126) and

$$\bar{a}_{AT,i}=\frac{1}{4\sqrt{2}}\left[1+\left(1-k_i^c\right)u_i\right][1+a_4\phi(1-\phi)][(1-h_{\rm inv})q_a+1+h_{\rm inv}]\left(\frac{1-q_{s,i}}{q_{c,i}}\right). \tag{137}$$

Equations (130) and (136) were discretized using a second-order finite difference scheme with grid spacing Δx and were solved using a first-order Euler scheme. The discretization of the diffusion flux with the tensor diffusivity in Eq. (136) was carried out in the same manner as in Appendix B of Ref. [31].

In this test, the spatial and time scales were normalized by d_0 and $d_0^2/D_{l,T}$, respectively. We employed a square computational box with an edge length of $5000d_0$. The simulations were carried out for a model alloy with $k_1^c=0.2$, $k_2^c=0.5$, $\mathrm{Le}_1=5.0$, $\mathrm{Le}_2=10.0$, $q_{s,T}=0.5$, $q_{s,1}=10^{-2}$, $q_{s,1}=10^{-3}$, $M_{u,1}=0.08$, $M_{u,2}=0.05$, and $\varepsilon_4=0.02$. The time step Δt was given as $\Delta t=\Delta x^2/(5D_T)$ and W_0 was set to $1.5\Delta x$. The number of spatial grid points was changed from 256^2 to 1536^2 and W_0/d_0 was accordingly changed from 29.30 to 4.88. A small half disk of a solid was initially placed at the origin of the x axis and the center of the y axis. The initial undercooling and supersaturation were set to $\theta=-0.5$ and $u_1=u_2=0.0$, respectively. The simulation was carried out until steady-state growth was achieved. Note that we employed the low Lewis numbers. This is because high Lewis numbers require a long time until steady-state growth is realized. In addition, to reduce the computational cost, the growth of the solid in the x direction was simulated by moving the computational box in the x direction along with the growth front of the solid. The simulation was accelerated by using a TESLA K40 graphics processing unit (GPU) [21–23].

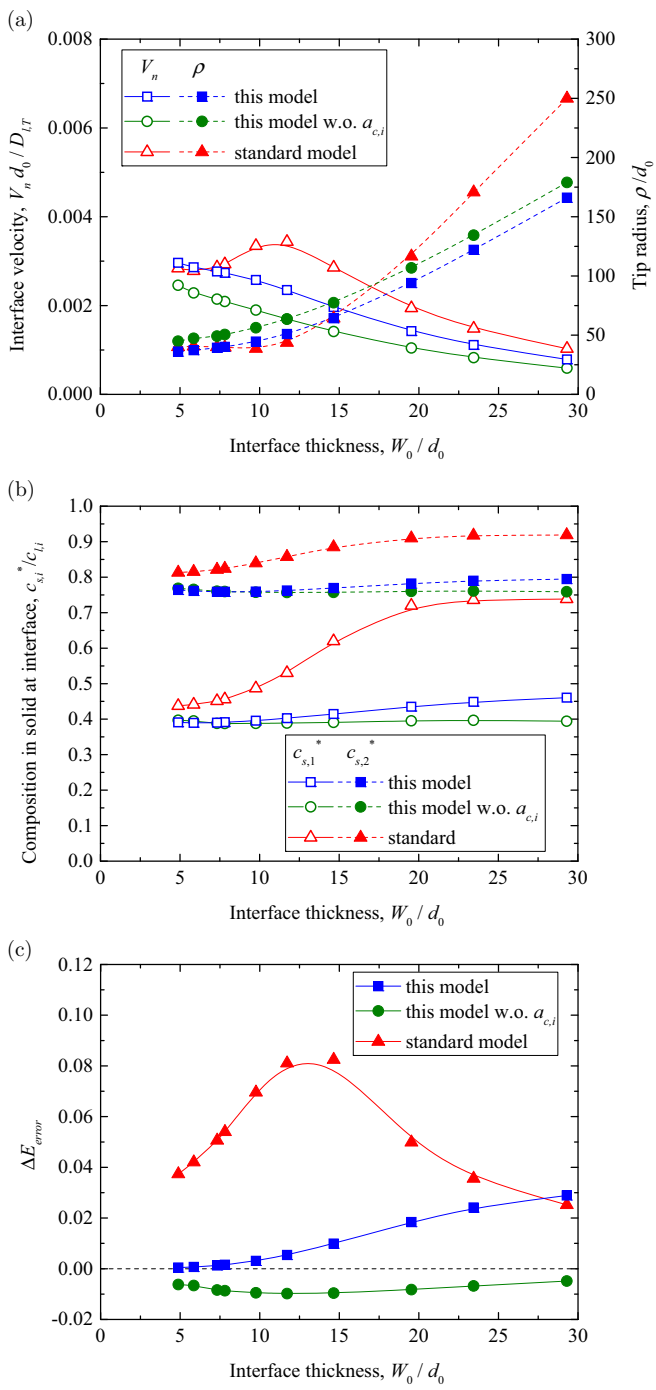

FIG. 2. (a) Convergence behavior of (a) the interface velocity (open plots) and the tip radius (filled plots), (b) the compositions in the solid near the dendrite tip, $c_{s,1}^*$ and $c_{s,2}^*$ ($\phi \approx 0.99$), and (c) error in the Gibbs-Thomson relation, calculated by the present model (squares), the present model without cross-coupling terms in ϕ equation (circles), and the standard model (triangles).

Figure 2 shows the results of the convergence test. The calculated dendrite tip velocity V_n and tip radius ρ are shown in Fig. 2(a) and the compositions of the solid behind the tip $c_{s,i}^*$ are presented in Fig. 2(b). The tip radius ρ was calculated by fitting the $\phi = 0$ contour at the dendrite tip to a parabola. Figure 2(c) shows the error in Gibbs-Thomson relation ΔE_{error} which is given as [15,27,31]

$$\Delta E_{\text{error}} = \sum_i M_{u,i} u_i^* + \frac{d_0(1 - 15\varepsilon_4)}{\rho}, \tag{138}$$

where u_i^* is a value of u_i evaluated at $\phi \approx 0.99$. The results of the present model are indicated by square plots (this model). We compare the results of this model and a standard model. The standard model corresponds to the present model without the coupling term in the ϕ equation [the last term in Eq. (130)] and the antitrapping current in the diffusion equation. More specifically, $a_I = 0$ and accordingly $\bar{a}_{c,i} = 0$ in Eq. (130) and $\bar{a}_{AT,i} = 0$ in Eq. (136). Also, the diffusivity $\mathbf{D}_i$ is the scalar as given by $D_i = [(1+\phi)k_i^c D_{s,i} + (1-\phi)D_{l,i}]/2$ in the standard model. Therefore, the standard model suffers from abnormal interface effects. The results of the standard model are indicated by triangle plots. In Fig. 2(a), V_n and ρ calculated by the present nonvariational model show monotonic convergence. Although they do not yet completely converge, the change of V_n and ρ are not significant when W_0/d_0 is small. On the other hand, V_n of the standard model exhibits nonmonotonic behavior, which stems from abnormal interface effects. A significant difference between the present nonvariational model and the standard model appear for $c_{s,i}^*$ in Fig. 2(b), which is sensitive to the abnormal interface effect originating from the discontinuity of the diffusion potential. The calculated $c_{s,i}^*$ of the standard model deviates from the well-converged values obtained by the present nonvariational model even for the smallest value of W_0/d_0. Furthermore, the large error exists in the Gibbs-Thomson relation in the case of the standard model even for the smallest value of W_0/d_0, which is in marked contrast to the result of the present nonvariational model. Hence, this numerical test shows that the performance of the present nonvariational model is much better than that of the standard model.

To understand the importance of the cross-coupling term in the ϕ equation, the same simulations were carried out by means of the present model without the cross-coupling term as specified by "this model w.o. $a_{c,i}$" (circle plots) in Fig. 2. The results of this model w.o. $a_{c,i}$ obviously differ from those of the present nonvariational model. V_n and ρ of the former model are always lower and larger than those of the latter model, respectively. Although the differences in $c_{s,i}$ between these models are small, the notable error still exists in the Gibbs-Thomson relation in the case of this model w.o. $a_{c,i}$ even for the smallest value of W_0/d_0. It is consistent with the result of the matched asymptotic analysis that a constant error appears in the Gibbs-Thomson relation without the cross-coupling term in the ϕ equation. This comparison indicates that the addition of the cross-coupling term improves the numerical accuracy.

Figure 2 demonstrates that the present nonvariational model exhibits good numerical performance by comparison to the other models. As already described, the numerical accuracy of the nonvariational model depends on the choice of the forms of $h(\phi)$, $h_{\text{inv}}(\phi)$, $f_{ac}(\phi)$, and $f_{\tau,ij}(\phi)$. Here we tested the accuracy of only one nonvariational model. Numerical testing of the nonvariational models with different sets of these functions may reveal the model which yields the highest accuracy as was carried out for the one-sided model [40]. This is one of

the important works tackled for practical use of the quantitative phase-field model.

VI. CONCLUSIONS

In this study, we have demonstrated a variational formulation of a quantitative phase-field model for nonisothermal solidification in a multicomponent alloy with two-sided asymmetric diffusion. The essential point of this procedure is that the diffusion fluxes of the conserved variables in the solid and liquid are separately formulated in the variational manner from the entropy functional, which is followed by the introduction of the local equilibrium conditions. In this procedure, the cross-coupling terms naturally arise in the ϕ equation and diffusion equation, one of which corresponds to the antitrapping current phenomenologically introduced in early models. Owing to both the coupling terms, this model becomes equivalent to the sharp-interface free-boundary problem of solidification in the thin-interface limit. This model is applicable to many practical problems because approximations and simplifications are not formally introduced into the bulk's free energy densities and off-diagonal elements of the diffusivity matrix are explicitly considered in this model. Furthermore, we have shown the nonvariational form of the present model which is more advantageous for numerical implementation than those in the previous study [31]. The numerical test of the model for nonisothermal solidification in a ternary alloy showed fast convergence of the results with decreasing interface thickness, i.e., good numerical performance.

Phase-field models generally require a high computational cost, which has imposed restrictions on their application. However, recent advances in high-performance computing techniques have enabled large-scale phase-field simulations of the competitive growth of a bunch of dendrites [21–23,43,44]. Furthermore, molecular dynamics (MD) simulations have contributed to the estimation of the interfacial properties required for quantitative phase-field simulations [45,46] and large-scale MD simulations are now closing the gap in the knowledge between the microstructural and atomistic scales [47,48]. We believe that, coupled with these recent advances, the present quantitative phase-field model will contribute to further progress in our understanding of the formation processes of solidification microstructures.

ACKNOWLEDGMENTS

This research was supported by a Grant-in-Aid for Scientific Research (B) (JSPS KAKENHI Grant No. 16H04541) from Japan Society for the Promotion of Science (JSPS) and the High Performance Computing Infrastructure (HPCI) in Japan. It was also supported in part by MEXT as a social and scientific priority issue (Creation of new functional devices and high-performance materials to support next-generation industries) to be tackled using the post-K computer.

APPENDIX A: TRANSFORMATION FOR $M_{n,ik'}$

The transformation for $M_{n,ik'}$ shown in Eq. (51) is explained here. First, note that a constant a and a regular matrix $\mathbf{A}$ obeys the relation $(a\mathbf{A})^{-1} = (1/a)\mathbf{A}^{-1}$. Also, the sum of regular matrices $\mathbf{A}$ and $\mathbf{B}$ satisfies the following relation:

$$(\mathbf{A}+\mathbf{B})^{-1} = \mathbf{A}^{-1}(\mathbf{A}^{-1}+\mathbf{B}^{-1})^{-1}\mathbf{B}^{-1}. \tag{A1}$$

Hence, the inverse matrix of $M_{c,ij}$ is written as

$$\begin{aligned} M_{c,ij}^{-1} &= \left(\frac{1-g}{2}M_{s,ij} + \frac{1+g}{2}M_{l,ij}\right)^{-1} = \sum_{k,k'} \frac{2}{1-g}M_{s,ik}^{-1}\left(\frac{2}{1-g}M_{s,kk'}^{-1} + \frac{2}{1+g}M_{l,kk'}^{-1}\right)^{-1}\frac{2}{1+g}M_{l,k'j}^{-1} \\ &= \sum_{k,k'} M_{s,ik}^{-1}\left(\frac{1+g}{2}M_{s,kk'}^{-1} + \frac{1-g}{2}M_{l,kk'}^{-1}\right)^{-1} M_{l,k'j}^{-1}. \end{aligned} \tag{A2}$$

Therefore, by substituting Eq. (A2) into Eq. (51), one obtains the following relation:

$$M_{n,ik'} = \sum_{j,k}\left(\frac{1+g}{2}M_{s,ij}M_{c,jk}^{-1}M_{l,kk'} + \frac{1-g}{2}M_{s,kk'}M_{c,jk}^{-1}M_{l,ij}\right) = \left(\frac{1+g}{2}M_{s,ik'}^{-1} + \frac{1-g}{2}M_{l,ik'}^{-1}\right)^{-1}. \tag{A3}$$

APPENDIX B: DETAILS OF THE MATCHED ASYMPTOTIC ANALYSIS

Some details of the matched asymptotic analysis are explained in this appendix. As described in Sec. III, $\phi_0(\eta) = -\tanh(\eta/\sqrt{2})$ and $c_{l,i,0} = C_{l,i,0}(s)$ are obtained from Eq. (72) at order ε^0 and from Eq. (73) at order ε^{-2}, respectively. The lowest-order expression of the Gibbs-Thomson relation Eq. (74) is obtained by integrating Eq. (72) at order ε^1 with respect to η after multiplying it by $\partial_\eta\phi_0$. Next, Eq. (73) at order ε^{-1} yields

$$\partial_\eta\left(\sum_j q_{ij}^n \partial_\eta c_{l,j,1}\right) - v_n \Delta C_i \frac{h'}{2}\partial_\eta\phi_0 + v_n\partial_\eta(a_{AT,i}\,\partial_\eta\phi_0) = 0, \tag{B1}$$

where the dependencies of quantities on ϕ_0 and $C_{i,0}$ such as $q_{ij} = q_{ij}(\phi_0,\{C_{k,0}\})$ and $\Delta C_i = \Delta C_i(\{C_{l,j,0}\})$ are not explicitly denoted for convenience. By integrating Eq. (B1) once, one obtains

$$\sum_j q_{ij}^n \partial_\eta c_{l,j,1} = v_n \Delta C_i \frac{h-1}{2} - v_n a_{AT,i}\, \partial_\eta \phi_0 + \sum_j q_{ij}(+1)\, \partial_r C_{l,j,0}\big|^-, \tag{B2}$$

where the integral constant was determined using the matching condition for $\eta \to -\infty$ ($\phi_0 \to +1$). In the limit of $\eta \to +\infty$ ($\phi_0 \to -1$), Eq. (B2) yields the following relation:

$$v_n \Delta C_i(\{C_{l,i,0}\}) = \sum_j q_{ij}(+1,\{C_{l,i,0}\})\, \partial_r C_{l,j,0}|^- - \sum_j q_{ij}(-1,\{C_{l,i,0}\})\, \partial_r C_{l,j,0}|^+. \tag{B3}$$

This equation is exactly the same as Eq. (75). Also, by substituting Eq. (67) into Eq. (B2), one obtains

$$\sum_j q_{ij}^n(\phi_0)\partial_\eta c_{l,j,1} = v_n \frac{h-1}{2}\left(\Delta C_i - \frac{1+h_{\rm inv}}{2}\sum_{j,k}(M_{l,ij} - M_{s,ij})M_{c,jk}^{-1}\Delta C_k\right) + \sum_j q_{ij}(+1)\partial_r C_{l,j,0}|^-, \tag{B4}$$

where the terms in the parenthesis in the first term can be rewritten as

$$\begin{aligned}\Delta C_i - \frac{1+h_{\rm inv}}{2}\sum_{j,k}(M_{l,ij} - M_{s,ij})M_{c,jk}^{-1}\Delta C_k &= \sum_{j,k}\Delta C_k M_{c,ij} M_{c,jk}^{-1} - \frac{1+h_{\rm inv}}{2}\sum_{j,k}(M_{l,ij} - M_{s,ij})M_{c,jk}^{-1}\Delta C_k \\ &= \sum_{j,k} M_{s,ij} M_{c,jk}^{-1}\Delta C_k.\end{aligned} \tag{B5}$$

Hence,

$$\sum_j q_{ij}^n(\phi_0)\partial_\eta c_{l,j,1} = v_n \frac{h-1}{2}\sum_{j,k} M_{s,ij} M_{c,jk}^{-1}\Delta C_k + \sum_j q_{ij}(+1)\partial_r C_{l,j,0}|^-. \tag{B6}$$

Furthermore, using the definition of q_{ij}^n, Eq. (B6) is rewritten as

$$-\frac{1}{D_{l,0}}\sum_j \chi_{l,k'j}\partial_\eta c_{l,j,1} = v_n \frac{h-1}{2}\sum_{i,j,k} M_{n,k'i}^{-1} M_{s,ij} M_{c,jk}^{-1}\Delta C_k + \sum_{i,j} M_{n,k'i}^{-1} q_{ij}(+1)\partial_r C_{l,j,0}|^-. \tag{B7}$$

Here, the following equation is obtained from Eqs. (A2) and (A3):

$$\sum_{i,j,k} M_{n,k'i}^{-1} M_{s,ij} M_{c,jk}^{-1}\Delta C_k = \sum_k M_{l,k'k}^{-1}\Delta C_k. \tag{B8}$$

By using Eq. (B8) and by rearranging the subscripts, one obtains

$$-\frac{1}{D_{l,0}}\sum_j \chi_{l,ij}\partial_\eta c_{l,j,1} = v_n \frac{h-1}{2}\sum_j M_{l,ij}^{-1}\Delta C_j + \sum_{j,k} M_{n,ij}^{-1} q_{jk}(+1)\partial_r C_{l,k,0}|^-. \tag{B9}$$

The integration of Eq. (B9) yields

$$-\frac{1}{D_{l,0}}\sum_j \chi_{l,ij} c_{l,j,1} = v_n \sum_j M_{l,ij}^{-1}\Delta C_j \int_0^\eta \frac{h-1}{2} d\xi + \sum_{j,k} q_{jk}(+1)\partial_r C_{l,k,0}|^- \int_0^\eta M_{n,ij}^{-1}(\phi_0) d\xi + A_{i,0}, \tag{B10}$$

where $A_{i,0}$ is the integral constant. By considering the matching condition in the limits of $\eta \to \pm\infty$ and the Stefan condition given by Eq. (B3), one obtains the following relation:

$$-\frac{1}{D_{l,0}}\sum_j \chi_{l,ij}\, C_{l,j,1}\big|^\pm = \frac{1}{2} v_n \sum_j M_{l,ij}^{-1}\Delta C_j H^\pm + \sum_{j,k} G_{ij}^\pm q_{jk}(+1)\, \partial_r C_{l,k,0}\big|^- + A_{i,0}, \tag{B11}$$

where $H^\pm$ and $G_{ij}^\pm$ are given by Eqs. (77) and (78), respectively. In the variational model, $H^+ = H^-$ and $G_{ij}^+ = G_{ij}^-$ are satisfied because $h = h_{\rm inv} = g$. Furthermore, these requirements can be satisfied when h and $h_{\rm inv}$ are an odd function of ϕ.

Next, the following relation is derived by integrating Eq. (72) at order ε^2 after multiplying by $\partial_\eta\phi_0$ and by considering the symmetry of the functions in the same manner as discussed in Refs. [14,24]:

$$\begin{aligned}&\frac{a_1}{\chi_e}\sum_i \frac{\partial \Delta G_{\rm driv}}{\partial c_{l,i}}\int_{-\infty}^{+\infty} c_{l,i,1}\widetilde{g}'(\phi_0)\partial_\eta\phi_0 d\xi - \int_{-\infty}^{+\infty}\sum_i a_{c,i}(\phi_0)\partial_\eta c_{l,i,1}\partial_\eta\phi_0 d\xi \\ &\quad - v_n\int_{-\infty}^{+\infty}\sum_{i,j}\alpha_{ij}(\phi_0)\Delta C_i M_{c,ij}^{-1}\Delta C_j(\partial_\eta\phi_0)^2 d\xi = 0.\end{aligned} \tag{B12}$$

By substituting Eq. (B10), Eqs. (63), and (70) into Eq. (B12), one obtains the following relation:

$$\begin{aligned}\sum_{i,j}\frac{\partial\Delta G_{\rm driv}}{\partial c_{l,i}}\chi^{-1}_{l,ij}A_{j,0} &= v_n\frac{1}{2J}\sum_{i,j,k}\frac{\partial\Delta G_{\rm driv}}{\partial c_{l,i}}\chi^{-1}_{l,ij}M^{-1}_{l,jk}\Delta C_k K+\frac{1}{J}\sum_{i,j,k,k'}\frac{\partial\Delta G_{\rm driv}}{\partial c_{l,i}}\chi^{-1}_{l,ij}Q_{jk}q_{kk'}(+1)\,\partial_r C_{l,k',0}\big|^-\\ &+v_n\frac{a_I}{I}T_0\int_{-\infty}^{+\infty}\sum_{i,j,k,k'}\Delta C_i M^{-1}_{c,ij}(M_{l,jk}-M_{s,jk})M^{-1}_{l,kk'}\Delta C_{k'}f_{ac}(\phi)\frac{h-1}{2}\frac{(1-h_{\rm inv})(1+h)}{4}d\xi\\ &+\frac{a_I}{I}T_0\sum_{i,j,k}\Delta C_i\big(M^{-1}_{s,ij}-M^{-1}_{l,ij}\big)q_{jk}(+1)\partial_r C_{l,k,0}|^-\int_{-\infty}^{+\infty}f_{ac}(\phi)\frac{(1-h_{\rm inv})(1+h)}{4}d\xi\\ &+\frac{a_I}{I}v_nT_0\int_{-\infty}^{+\infty}\sum_{i,j}\Delta C_i M^{-1}_{c,ij}\Delta C_j f_{\tau,ij}(\phi)\frac{1-h^2}{4}d\xi,\end{aligned}\tag{B13}$$

where K is given by Eq. (82) and

$$Q_{jk}=\int_{-\infty}^{+\infty}\left[\int_0^{\eta}M^{-1}_{n,jk}d\xi\right]\widetilde{g}'(\phi_0)\partial_\eta\phi_0 d\xi.\tag{B14}$$

Here, note that the following relation is always satisfied:

$$\frac{\partial\Delta G_{\rm driv}}{\partial c_{l,i}}=-T_0\frac{\partial}{\partial c_{l,i}}\left(s_{s,\rm bulk}-s_{l,\rm bulk}-\sum_{j=1}^{n+1}(c_{s,j}-c_{l,j})\Delta s_{c,j}\right)=-T_0\left(\sum_j\Delta C_j\chi_{l,ji}\right).\tag{B15}$$

Then, one can obtain Eq. (84). By combining Eqs. (B11), (B13), and (84), the following relation can be obtained:

$$\begin{aligned}\frac{1}{T_0D_{l,0}}\sum_i\frac{\partial\Delta G_{\rm driv}}{\partial c_{l,i}}C_{l,i,1}\big|^{\pm} &= v_n\sum_{i,j}\Delta C_i M^{-1}_{l,ij}\Delta C_j\left(\frac{JH^{\pm}+K}{2J}\right)\\ &-v_n\frac{a_I}{I}\int_{-\infty}^{+\infty}\sum_{i,j,k,k'}\Delta C_i M^{-1}_{c,ij}(M_{l,jk}-M_{s,jk})M^{-1}_{l,kk'}\Delta C_{k'}f_{ac}(\phi)\frac{h-1}{2}\frac{(1-h_{\rm inv})(1+h)}{4}d\xi\\ &-v_n\frac{a_I}{I}\int_{-\infty}^{+\infty}\sum_{i,j}\Delta C_i M^{-1}_{c,ij}\Delta C_j\frac{1-h^2}{4}f_{\tau,ij}(\phi)d\xi\\ &+\sum_{i,j,k}\Delta C_i G^{\pm}_{ij}q_{jk}(+1)\,\partial_r C_{l,k,0}\big|^-+\frac{1}{J}\sum_{i,j,k}\Delta C_i Q_{ij}q_{jk}(+1)\,\partial_r C_{l,k,0}\big|^-\\ &-\frac{a_I}{I}\sum_{i,j,k}\Delta C_i\big(M^{-1}_{s,ij}-M^{-1}_{l,ij}\big)\,q_{jk}(+1)\,\partial_r C_{l,k,0}\big|^-\int_{-\infty}^{+\infty}f_{ac}(\phi)\frac{(1-h_{\rm inv})(1+h)}{4}d\xi.\end{aligned}\tag{B16}$$

The right-hand side of Eq. (B16) consists of terms proportional to v_n and $q_{jk}(+1)\partial_r C_{l,k,0}|^-$. In the previous models without the cross-coupling term in the ϕ equation (i.e., the models with $a_{c,i}=0$), the latter terms appear in the Gibbs-Thomson relation, causing the unphysical magnification of the interface effect. In the present model, on the other hand, the terms proportional to $q_{jk}(+1)\partial_r C_{l,k,0}|^-$ can be canceled out when the following relation is satisfied:

$$\frac{a_I}{I}\big(M^{-1}_{s,ij}-M^{-1}_{l,ij}\big)\int_{-\infty}^{+\infty}f_{ac}(\phi)\frac{1-h_{\rm inv}}{2}\frac{1+h}{2}d\xi=G^{\pm}_{ij}+\frac{Q_{ij}}{J}.\tag{B17}$$

Here, Q_{ij} can be rewritten as

$$Q_{ij}=\int_{-\infty}^{+\infty}\left[\int_0^{\eta}M^{-1}_{n,ij}d\xi\right]\widetilde{g}'(\phi_0)\partial_\eta\phi_0 d\xi=\frac{J}{2}\big(M^{-1}_{l,ij}-M^{-1}_{s,ij}\big)\int_0^{+\infty}(h_{\rm inv}+1)d\xi+\frac{J}{4}\big(M^{-1}_{l,ij}-M^{-1}_{s,ij}\big)\int_{-\infty}^{+\infty}(h_{\rm inv}g-1)d\xi,\tag{B18}$$

where we employed the fact that the integral of the odd function from $\eta=-\infty$ to $+\infty$ vanishes. By using Eqs. (B18) and (78), the right-hand side of Eq. (B17) is rewritten as

$$G^{\pm}_{ij}+\frac{Q_{ij}}{J}=\frac{1}{4}\big(M^{-1}_{l,ij}-M^{-1}_{s,ij}\big)\int_{-\infty}^{+\infty}(h_{\rm inv}g-1)d\xi.\tag{B19}$$

Hence, if the following relation is satisfied, the terms proportional to $q_{jk}(+1)\partial_r C_{l,k,0}|^-$ vanish in Eq. (B16):

$$a_I = I\int_{-\infty}^{+\infty}(1-h_{\rm inv}g)d\xi \Big/ \int_{-\infty}^{+\infty} f_{ac}(\phi)(1-h_{\rm inv})(1+h)d\xi. \tag{B20}$$

This relation is automatically satisfied in the variational model because $h_{\rm inv}=h=g$, $f_{ac}(\phi)=1$, and $a_I=I$. In the nonvariational model, a_I is determined by Eq. (B20). Now, Eq. (B16) is written as Eq. (79) and the Gibbs-Thomson relation is reproduced.

Finally, Eq. (73) at order ε^0 is given as

$$\begin{aligned}
&\partial_\eta\left(\sum_j q_{ij}^n\partial_\eta c_{l,j,2}\right)+\partial_\eta\left(\sum_j \frac{\partial q_{ij}^n}{\partial\phi}\phi_1\partial_\eta c_{l,j,1}\right)+\partial_\eta\left(\sum_{j,k}\frac{\partial q_{ij}^n}{\partial c_{l,k}}c_{l,k,1}\partial_\eta c_{l,j,1}\right)\\
&-\frac{1}{2}v_n\Delta C_i\partial_\eta\left(\frac{h'(\phi_0)}{2}\phi_1\right)+v_n\partial_\eta\left(\frac{1+h}{2}\sum_j k_{ij}^c c_{l,j,1}+\frac{1-h}{2}c_{l,i,1}\right)\\
&+v_n\partial_\eta(a_{AT,i}\,\partial_\eta\phi_1)+v_n\partial_\eta\left(\frac{\partial a_{AT,i}}{\partial\phi}\phi_1\,\partial_\eta\phi_0\right)+v_n\partial_\eta\left(\sum_j\frac{\partial a_{AT,i}}{\partial c_{l,j}}c_{l,j,1}\,\partial_\eta\phi_0\right)\\
&+\partial_s\left(\sum_j q_{ij}^t\partial_s C_{l,j,0}\right)+\kappa\sum_j q_{ij}^n\partial_\eta c_{l,j,1}+\kappa v_n a_{AT,i}\,\partial_\eta\phi_0=0.
\end{aligned}\tag{B21}$$

Integrating Eq. (B21) once yields

$$\begin{aligned}
&\sum_j q_{ij}^n\partial_\eta c_{l,j,2}+\sum_{j,k}\frac{\partial q_{ij}^n}{\partial c_{l,k}}c_{l,k,1}\partial_\eta c_{l,j,1}+v_n\frac{1+h}{2}\sum_j k_{ij}^c c_{l,j,1}+v_n\frac{1-h}{2}c_{l,i,1}\\
&+\sum_j\partial_s^2 C_{l,j,0}\int_0^\eta q_{ij}^t d\xi+\sum_{j,k}\partial_s C_{l,j,0}\partial_s C_{l,k,0}\int_0^\eta\frac{\partial q_{ij}^t}{\partial c_{l,k}}d\xi+\kappa\int_0^\eta\left(\sum_j q_{ij}^n\partial_\eta c_{l,j,1}+v_n a_{AT,i}\,\partial_\eta\phi_0\right)d\xi=A_{i,1},
\end{aligned}\tag{B22}$$

where $A_{i,1}$ is the integral constant. In Eq. (B22), we omitted the terms proportional to ϕ_1 and $\partial_\eta\phi_0$ because these terms are negligible in the limits of $\eta\to\pm\infty$. Using Eq. (B2), the last term on the right-hand side of Eq. (B22) is given in the limit of $\eta\to\pm\infty$ as

$$\kappa\int_0^{\pm\infty}\left(\sum_j q_{ij}\partial_\eta c_{l,j,1}+v_n a_{AT,i}\,\partial_\eta\phi_0\right)d\xi=\kappa\int_0^{\pm\infty}v_n\Delta C_i\frac{h\pm1}{2}d\xi+\kappa\sum_j q_{ij}(\mp1)\,\partial_r C_{l,j,0}\big|^{\pm}\eta. \tag{B23}$$

Also, the diffusion equation of the outer solution $C_{l,i,0}$ is expressed in the curvilinear coordinate as

$$v_n\partial_r C_{l,i,0}+\sum_j q_{ij}\partial_r^2 C_{l,j,0}+\sum_{j,k}\frac{\partial q_{ij}}{\partial C_{l,k}}\partial_r C_{l,k,0}\partial_r C_{l,j,0}+\kappa\sum_j q_{ij}\partial_r C_{l,j,0}+\partial_s\left(\sum_j q_{ij}\partial_s C_{l,j,0}\right)=0, \tag{B24}$$

where $q_{ij}=q_{ij}(+1)$ in the solid and $q_{ij}=q_{ij}(-1)$ in the liquid. Therefore, by taking the limit of Eq. (B22) for $\eta\to\pm\infty$ and calculating the difference between them, one obtains

$$\begin{aligned}
v_n C_{l,i,1}|^+-v_n\sum_j k_{ij}^c C_{l,j,1}|^- &= \sum_j q_{ij}(+1)\partial_r C_{l,j,1}|^-+\sum_{j,k}\frac{\partial q_{ij}(+1)}{\partial c_{l,k}}C_{l,k,1}|^-\partial_r C_{l,j,0}|^-\\
&\quad-\sum_j q_{ij}(-1)\partial_r C_{l,j,1}|^+-\sum_{j,k}\frac{\partial q_{ij}(-1)}{\partial c_{l,k}}C_{l,k,1}|^+\partial_r C_{l,j,0}|^+.
\end{aligned}\tag{B25}$$

This corresponds to Eq. (87) and is valid as long as Eqs. (88) and (89) are satisfied. From Eqs. (B3) and (B25), one can obtain Eq. (90), which corresponds to the Stefan condition.

[1] W. J. Boettinger, J. A. Warren, C. Beckermann, and A. Karma, Annu. Rev. Mater. Res. **32**, 163 (2002).

[2] I. Steinbach, Model. Simul. Mater. Sci. Eng. **17**, 073001 (2009).

[3] N. Provatas and K. Elder, *Phase-Field Methods in Materials Science and Engineering* (Wiley-VCH, New York, 2010).

[4] T. Takaki, ISIJ Int. **54**, 437 (2014).

[5] O. Penrose and P. C. Fife, Physica D **43**, 44 (1990).
[6] A. A. Wheeler, W. J. Boettinger, and G. B. McFadden, Phys. Rev. A **45**, 7424 (1992).
[7] S. L. Wang, R. F. Sekerka, A. A. Wheeler, B. T. Murray, S. R. Coriell, B. J. Braun, and G. B. McFadden, Physica D **69**, 189 (1993).
[8] J. A. Warren and W. J. Boettinger, Acta Metall. Mater. **43**, 689 (1995).
[9] I. Steinbach, F. Pezzolla, B. Nestler, M. Seeβelberg, R. Prieler, G. J. Schmitz, and J. L. L. Rezende, Physica D **94**, 135 (1996).
[10] S. G. Kim, W. T. Kim, and T. Suzuki, Phys. Rev. E **60**, 7186 (1999).
[11] R. F. Almgren, SIAM J. Appl. Math. **59**, 2086 (1999).
[12] A. Karma and W.-J. Rappel, Phys. Rev. E **57**, 4323 (1998).
[13] A. Karma, Phys. Rev. Lett. **87**, 115701 (2001).
[14] B. Echebarria, R. Folch, A. Karma, and M. Plapp, Phys. Rev. E **70**, 061604 (2004).
[15] J. C. Ramirez, C. Beckermann, A. Karma, and H.-J. Diepers, Phys. Rev. E **69**, 051607 (2004).
[16] R. Folch and M. Plapp, Phys. Rev. E **72**, 011602 (2005).
[17] S. G. Kim, Acta Mater. **55**, 4391 (2007).
[18] M. Greenwood, M. Haataja, and N. Provatas, Phys. Rev. Lett. **93**, 246101 (2004).
[19] J. Rosam, P. K. Jimack, and A. M. Mullis, Phys. Rev. E **79**, 030601(R) (2009).
[20] S. Gurevich, A. Karma, M. Plapp, and R. Trivedi, Phys. Rev. E **81**, 011603 (2010).
[21] T. Takaki, M. Ohno, T. Shimokawabe, and T. Aoki, Acta Mater. **81**, 272 (2014).
[22] T. Takaki, M. Ohno, Y. Shibuta, S. Sakane, T. Shimokawabe, and T. Aoki, J. Cryst. Growth **442**, 14 (2016).
[23] T. Takaki, S. Sakane, M. Ohno, Y. Shibuta, T. Shimokawabe, and T. Aoki, Acta Mater. **118**, 230 (2016).
[24] M. Ohno and K. Matsuura, Phys. Rev. E **79**, 031603 (2009).
[25] M. Ohno and K. Matsuura, Acta Mater. **58**, 5749 (2010).
[26] M. Ohno and K. Matsuura, Acta Mater. **58**, 6134 (2010).
[27] M. Ohno, Phys. Rev. E **86**, 051603 (2012).
[28] G. Boussinot and E. A. Brener, Phys. Rev. E **89**, 060402(R) (2014).
[29] E. A. Brener and G. Boussinot, Phys. Rev. E **86**, 060601(R) (2012).
[30] A. Fang and Y. Mi, Phys. Rev. E **87**, 012402 (2013).
[31] M. Ohno, T. Takaki, and Y. Shibuta, Phys. Rev. E **93**, 012802 (2016).
[32] J. Tiaden, B. Nestler, H. J. Diepers, and I. Steinbach, Physica D **115**, 73 (1998).
[33] M. Hillert, Acta Mater. **47**, 4481 (1999).
[34] I. Steinbach, L. Zhang, and M. Plapp, Acta Mater. **60**, 2689 (2012).
[35] H. Wang, F. Liu, G. J. Ehlen, and D. M. Herlach, Acta Mater. **61**, 2617 (2013).
[36] In the previous study [31], the reaction terms of $\partial_t c_p$ were taken into account for expression of free energy dissipation. However, as described in this paper, the reaction terms do not need to be introduced into Eq. (11). In Ref. [31], the reaction terms were neglected in the final form of the time evolution equations for ϕ; and a composition field and hence the final equations exhibit the correct forms.
[37] S. R. de Groot and P. Mazur, *Non-equilibrium Thermodynamics* (Dover, New York, 1983).
[38] M. Nicoli, M. Plapp, and H. Henry, Phys. Rev. E **84**, 046707 (2011).
[39] L. Kaufmann and H. Bernstein, *Computer Calculation of Phase Diagrams with Special Reference to Refractory Materials* (Academic, New York, 1970).
[40] M. Ohno, T. Takaki, and Y. Shibuta, J. Comput. Phys. **335**, 621 (2017).
[41] A. T. Dinsdale, CALPHAD **15**, 317 (1991).
[42] J. Eiken, B. Böttger, and I. Steinbach, Phys. Rev. E **73**, 066122 (2006).
[43] Y. Shibuta, M. Ohno, and T. Takaki, JOM **67**, 1793 (2015).
[44] T. Takaki, T. Shimokawabe, M. Ohno, A. Yamanaka, and T. Aoki, J. Cryst. Growth **382**, 21 (2013).
[45] Y. Shibuta, K. Oguchi, and M. Ohno, Scr. Mater. **86**, 20 (2014).
[46] M. Asta, C. Beckermann, A. Karma, W. Kurz, R. Napolitano, M. Plapp, G. Purdy, M. Rappaz, and R. Trivedi, Acta Mater. **57**, 941 (2009).
[47] Y. Shibuta, S. Sakane, T. Takaki, and M. Ohno, Acta Mater. **105**, 328 (2016).
[48] Y. Shibuta, S. Sakane, E. Miyoshi, S. Okita, T. Takaki and M. Ohno, Nat. Commun. **8**, 10 (2017).